SUPPORTING INFORMATION

Thiol-Ene Click-Inspired Late-Stage Modification of Long-Chain Polyurethane Dendrimers

Dhruba P. Poudel [1] and Richard T. Taylor [1,*]

[1] Department of Chemistry and Biochemistry, Miami University, Oxford, OH 45056, USA; poudeld@miamioh.edu
* Correspondence: taylorrt@miamioh.edu

Table of Contents

1. Extended structure of G1 – G3 dendrons and dendrimers

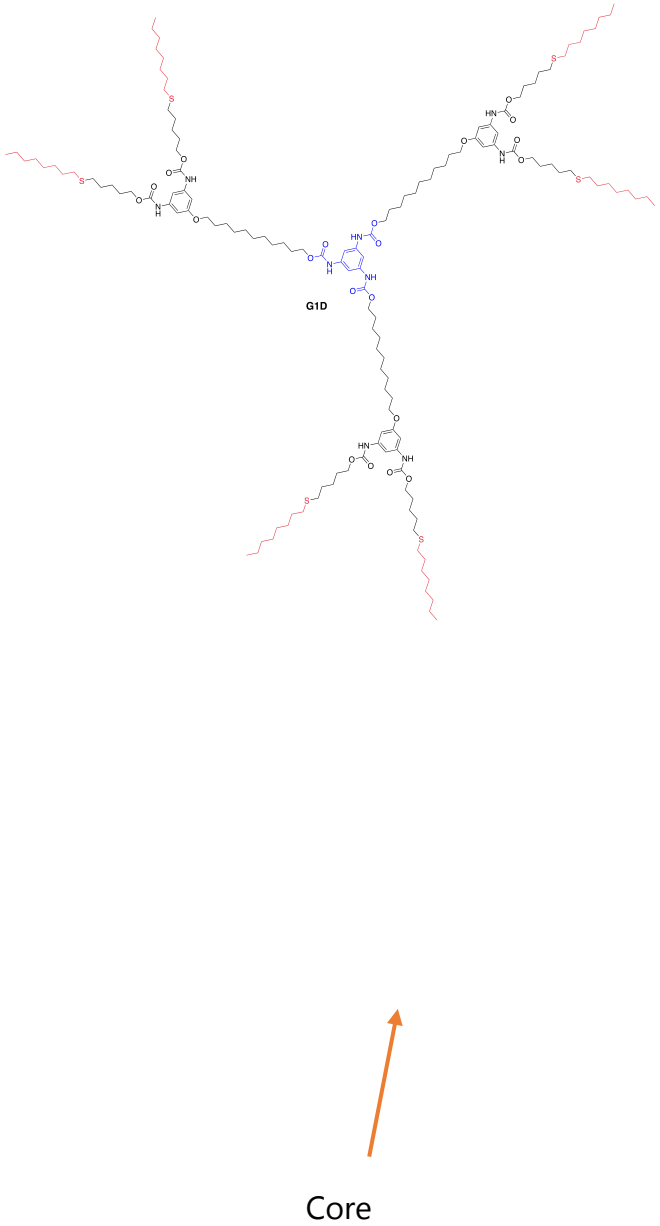

Figure S1. Expanded structure of thiol-ene functionalized **G1D** (*top*) and its ball and stick (3D, hydrogen atoms are removed) model with lowest energy (*bottom*, 457.9 kJ/mol at 298 K). Red = oxygen atom, blue = nitrogen atom, yellow = sulfur atom.

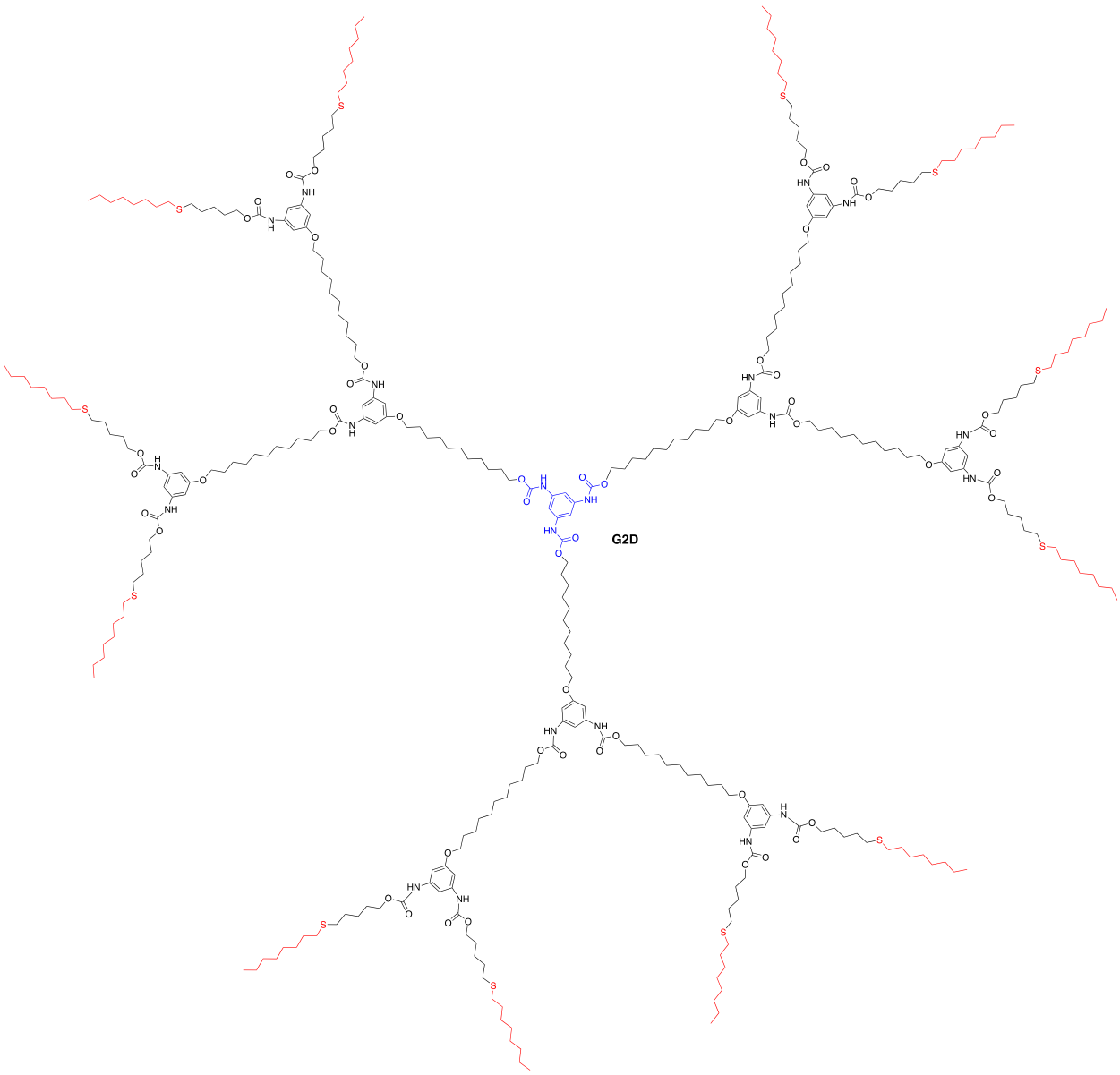

Figure S2. Expanded structure of thiol-ene functionalized **G2D**.

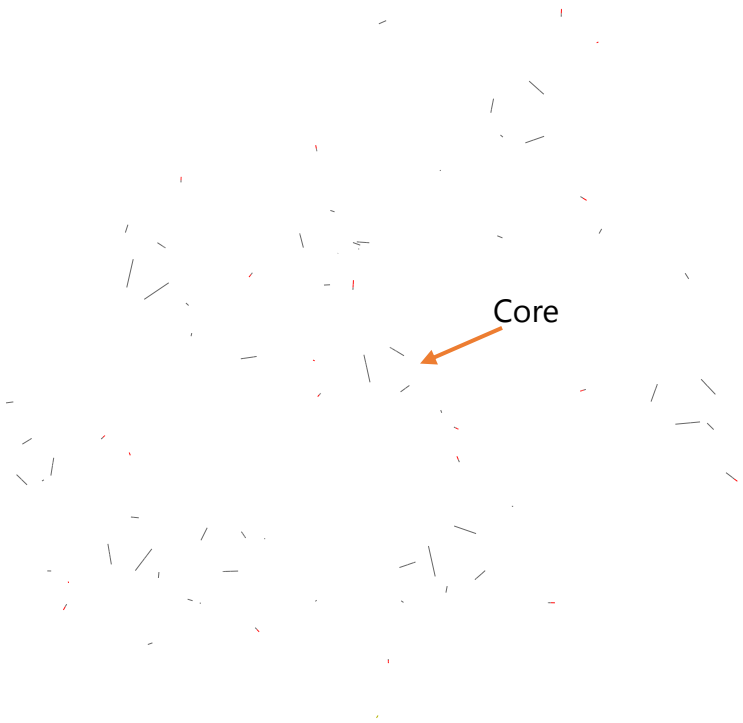

Figure S3. Optimized geometry (with the hydrogen atoms removed) of thiol-ene functionalized G2D showing 3D ball and stick model (E = 750.0 kJ/mol at 298 K). Red = oxygen atom, blue = nitrogen atom, yellow = sulfur atom.

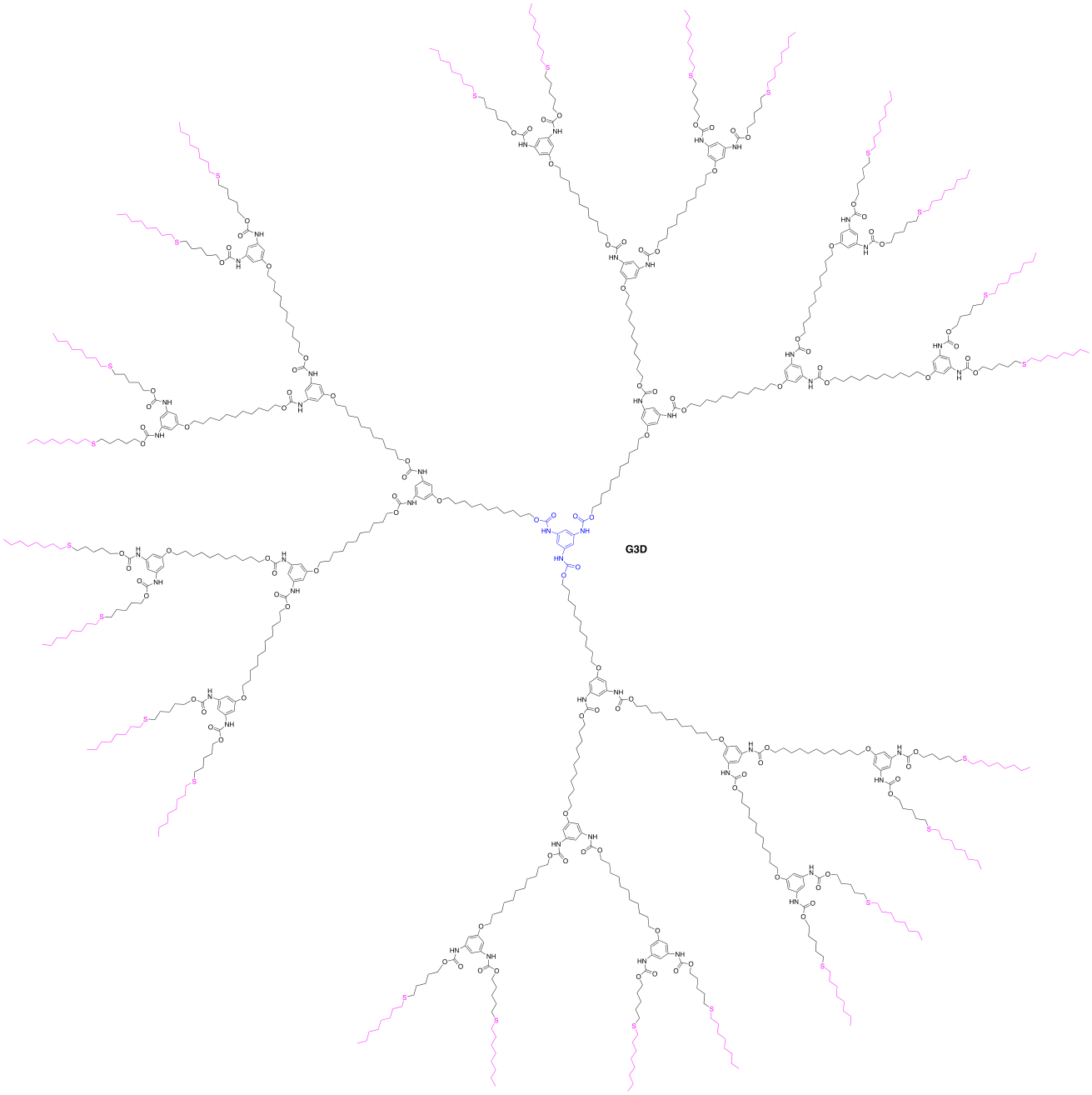

Figure S4. Expanded structure of thiol-ene functionalized **G3D**.

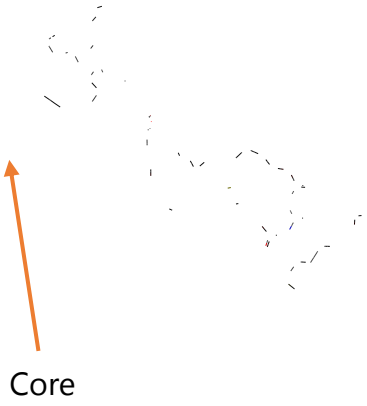

Figure S5. Optimized geometry (with the hydrogen atoms removed) of thiol-ene functionalized **G3D** showing 3D ball and stick model (E = 1735.4 kJ/mol at 298 K). Red = oxygen atom, blue = nitrogen atom, yellow = sulfur atom.

2. Copies of ^{1}H, ^{13}C NMR, and 2D spectra of G2 – G3 dendrons and dendrimers

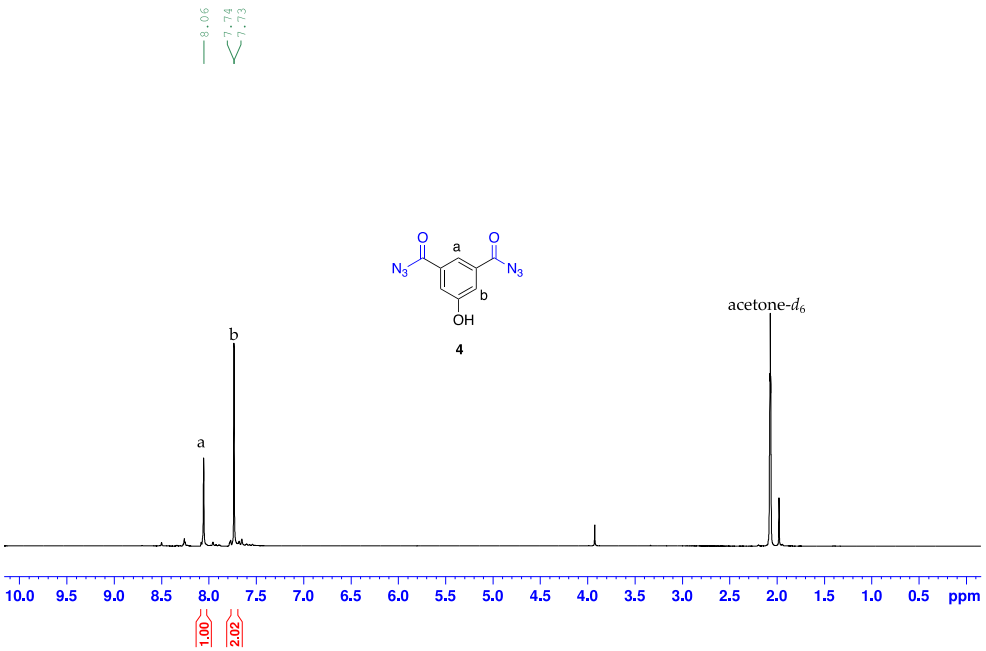

Figure S6. ^{1}H NMR spectrum (500 MHz, CD_3COCD_3, 298 K) of 5-hydroxy-1,3-benzenedicarbonyl diazide **4**.

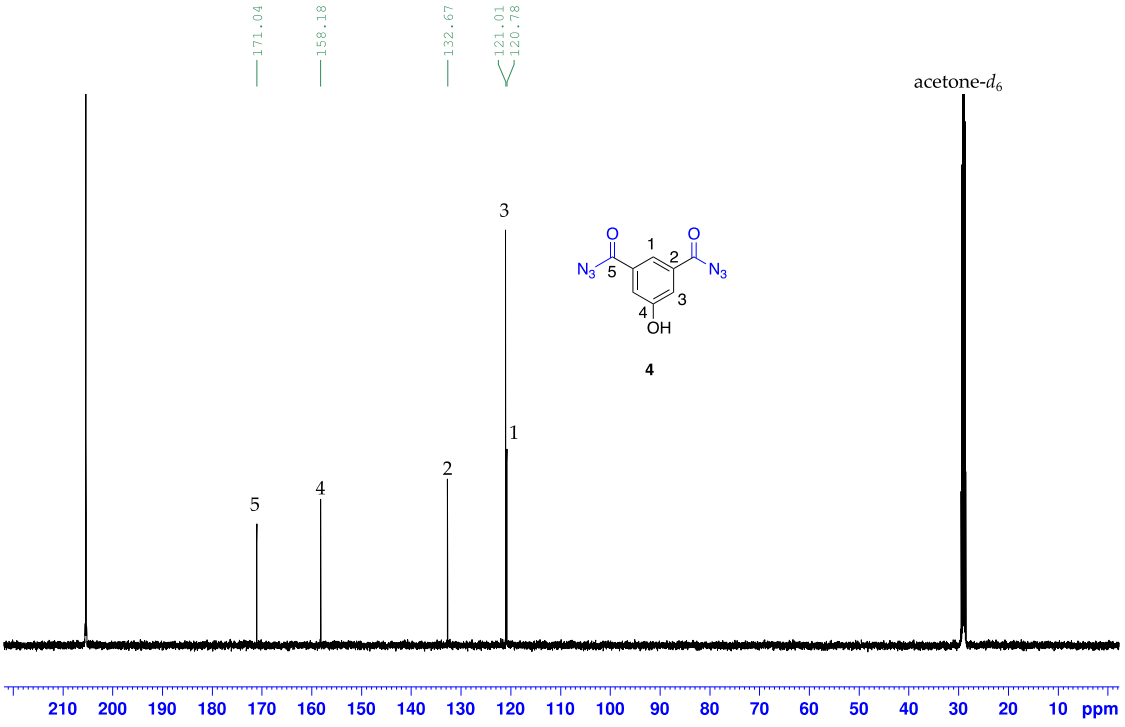

Figure S7. ^{13}C NMR spectrum (126 MHz, CD_3COCD_3, 298 K) of 5-hydroxy-1,3-benzenedicarbonyl diazide **4**.

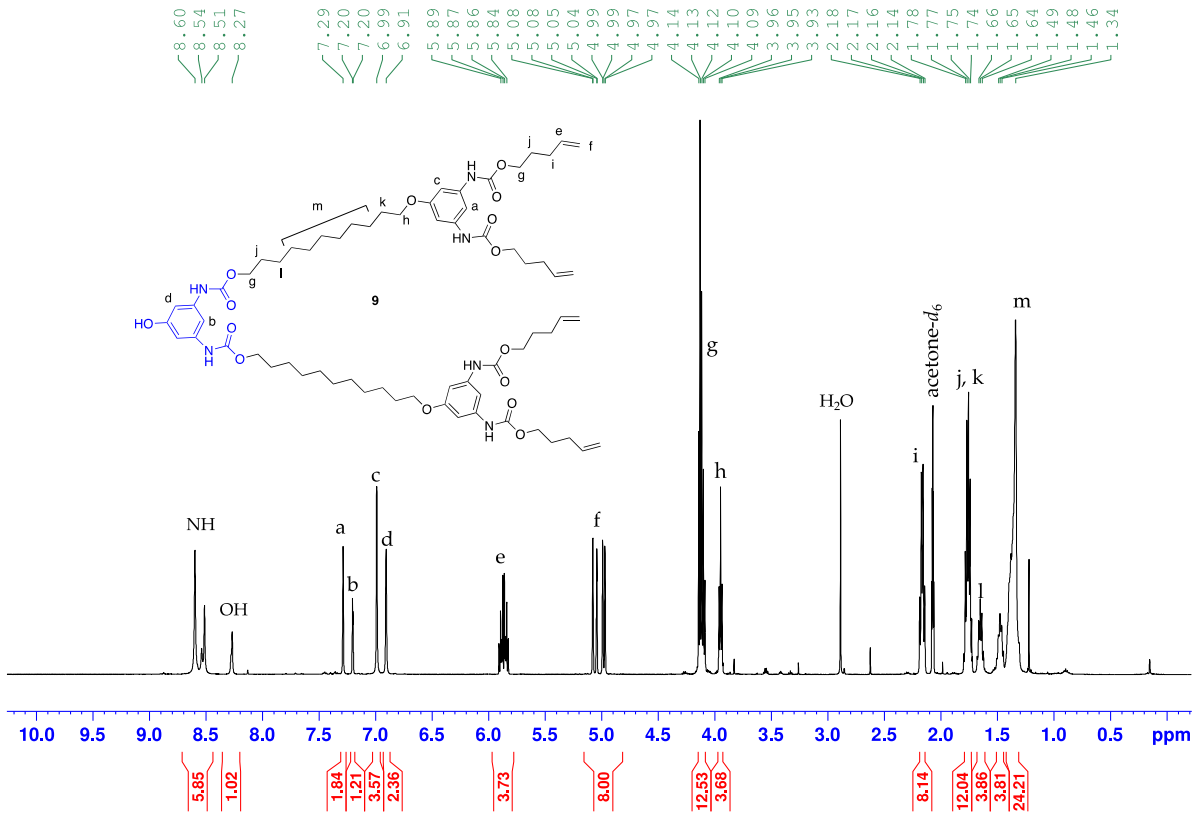

Figure S8. ^{1}H NMR spectrum (500 MHz, CD_3COCD_3, 298 K) of G2 phenolic wedge **9**.

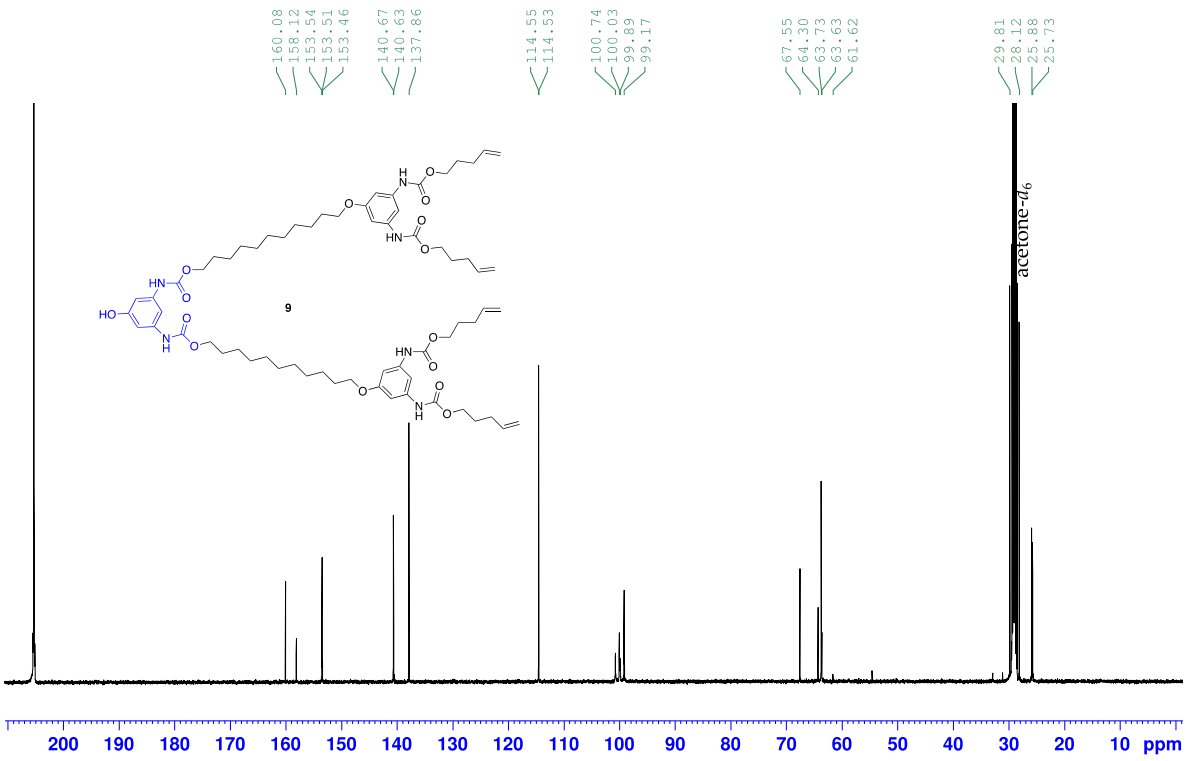

Figure S9. ^{13}C NMR spectrum (126 MHz, CD_3COCD_3, 298 K) of G2 phenolic wedge **9**.

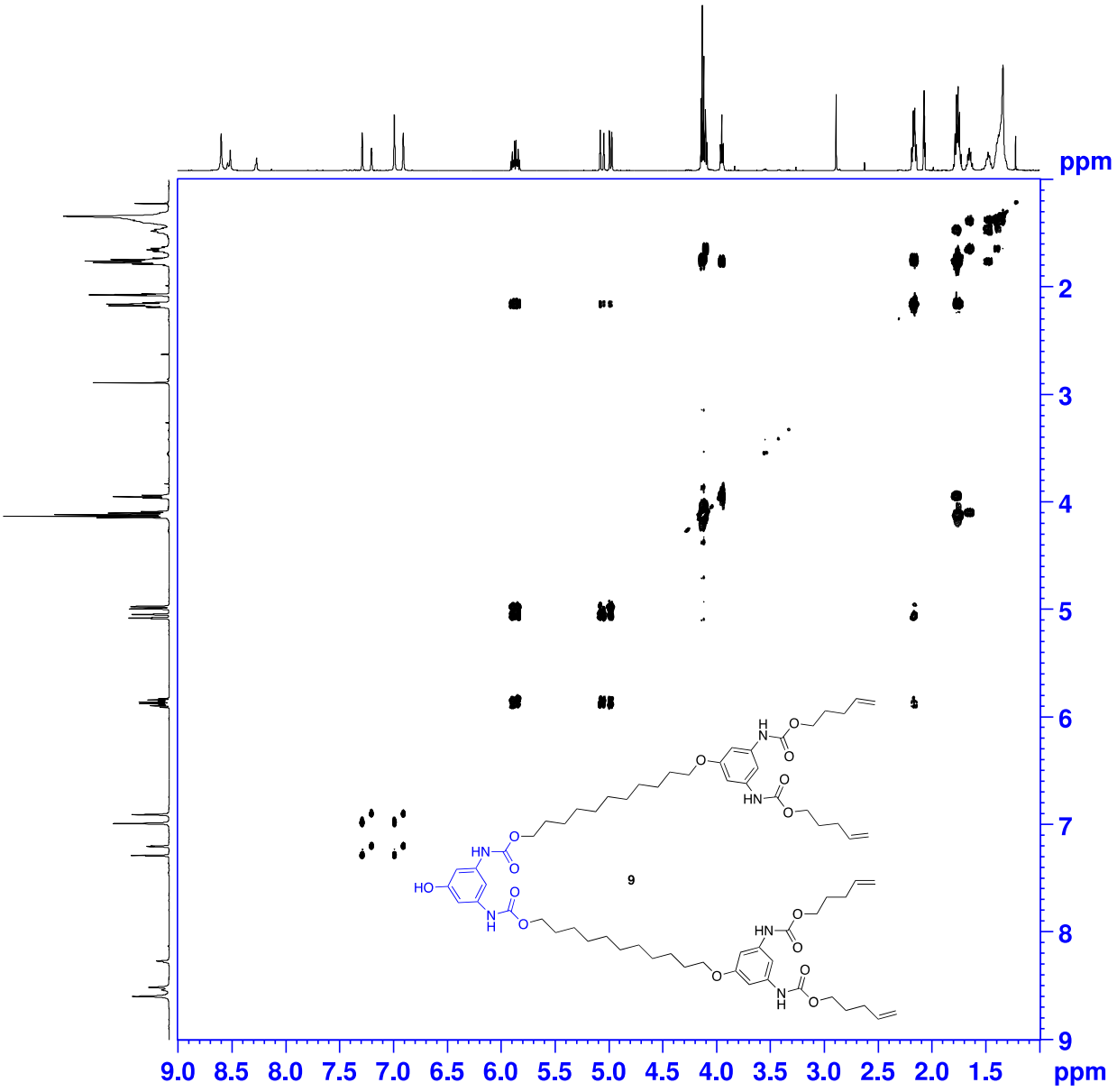

Figure S10. ^{1}H-^{1}H COSY spectrum (500 MHz, CD_3COCD_3, 298 K) of G2 phenolic wedge **9**.

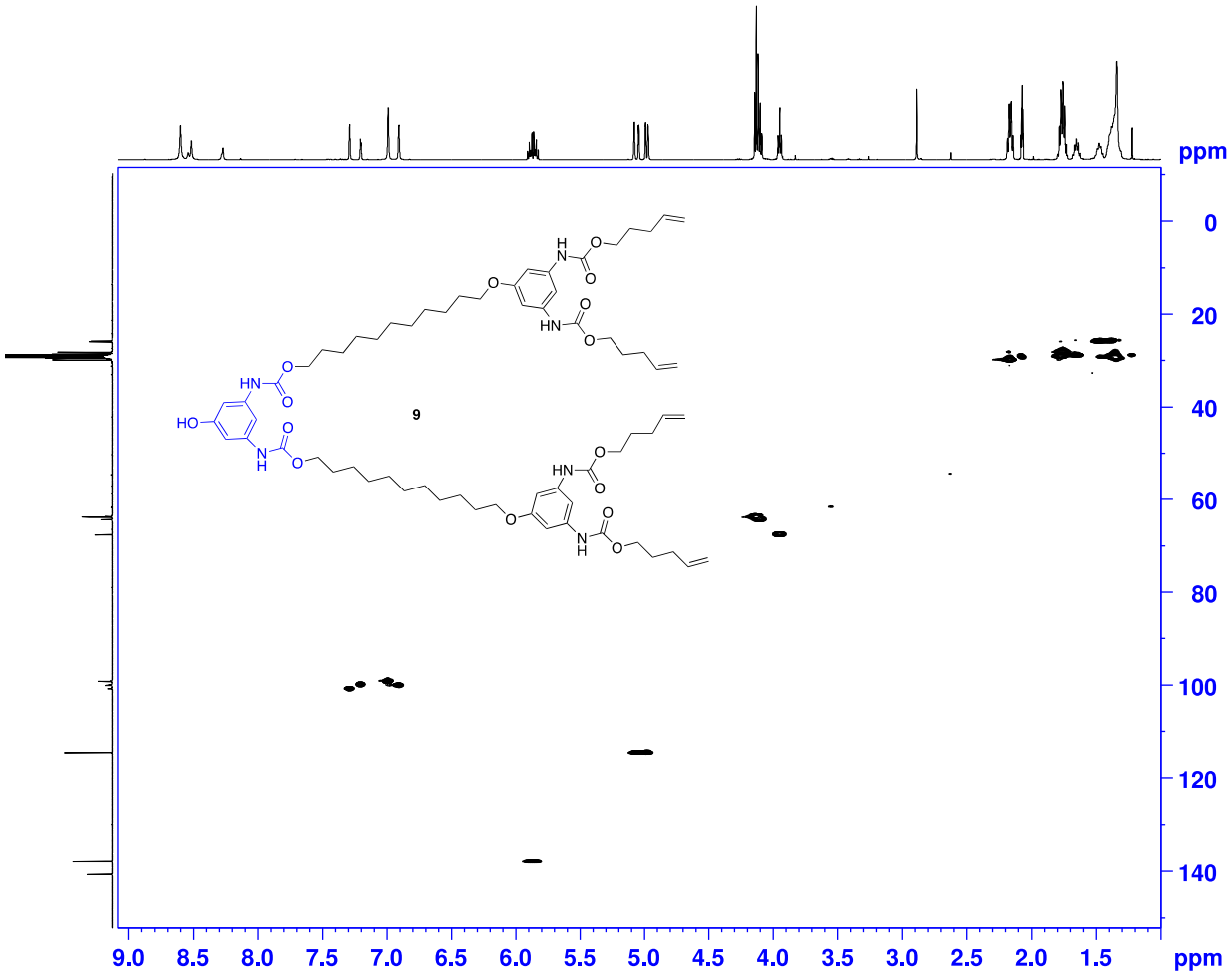

Figure S11. HSQC (^{1}H-^{13}C) spectrum (500 MHz, CD_3COCD_3, 298 K) of G2 phenolic wedge **9**.

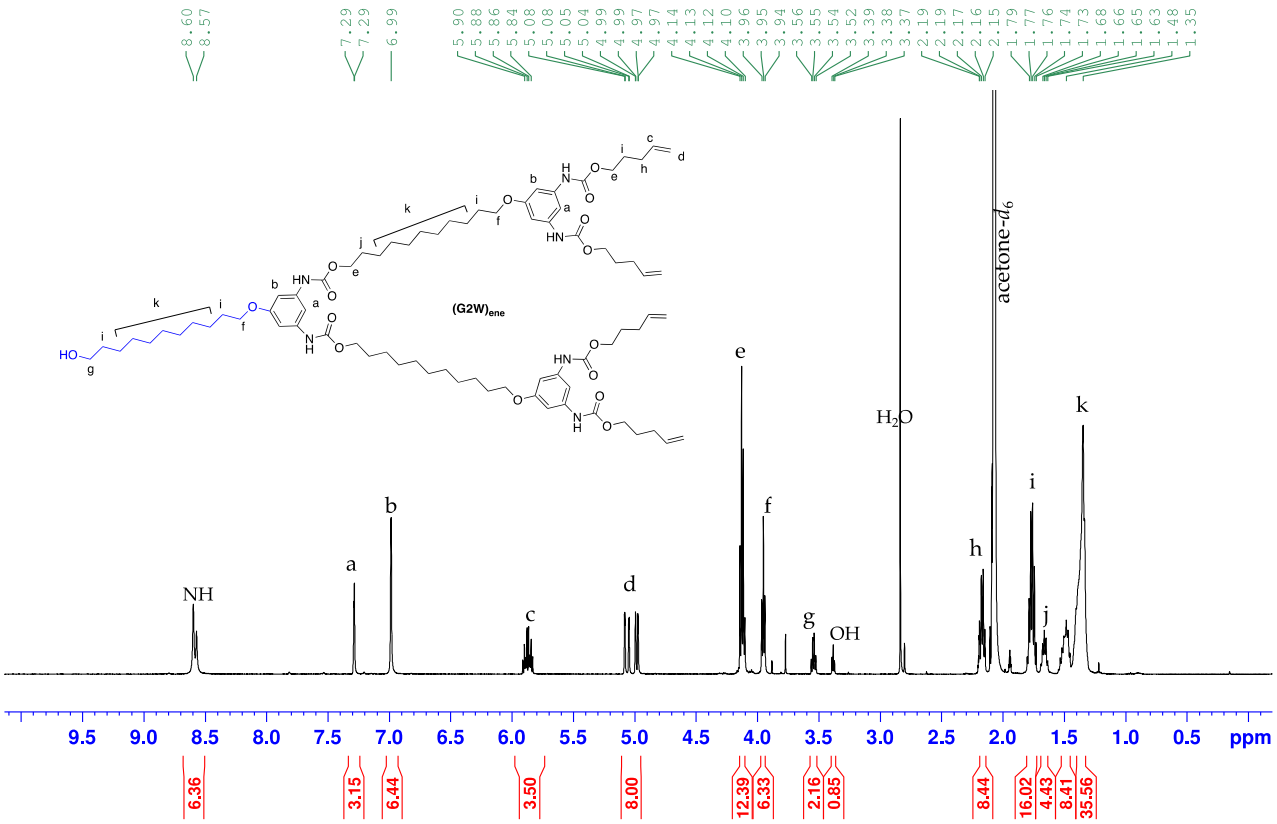

Figure S12. ^{1}H NMR spectrum (500 MHz, CD_3COCD_3, 298 K) of **(G2W)$_{ene}$**.

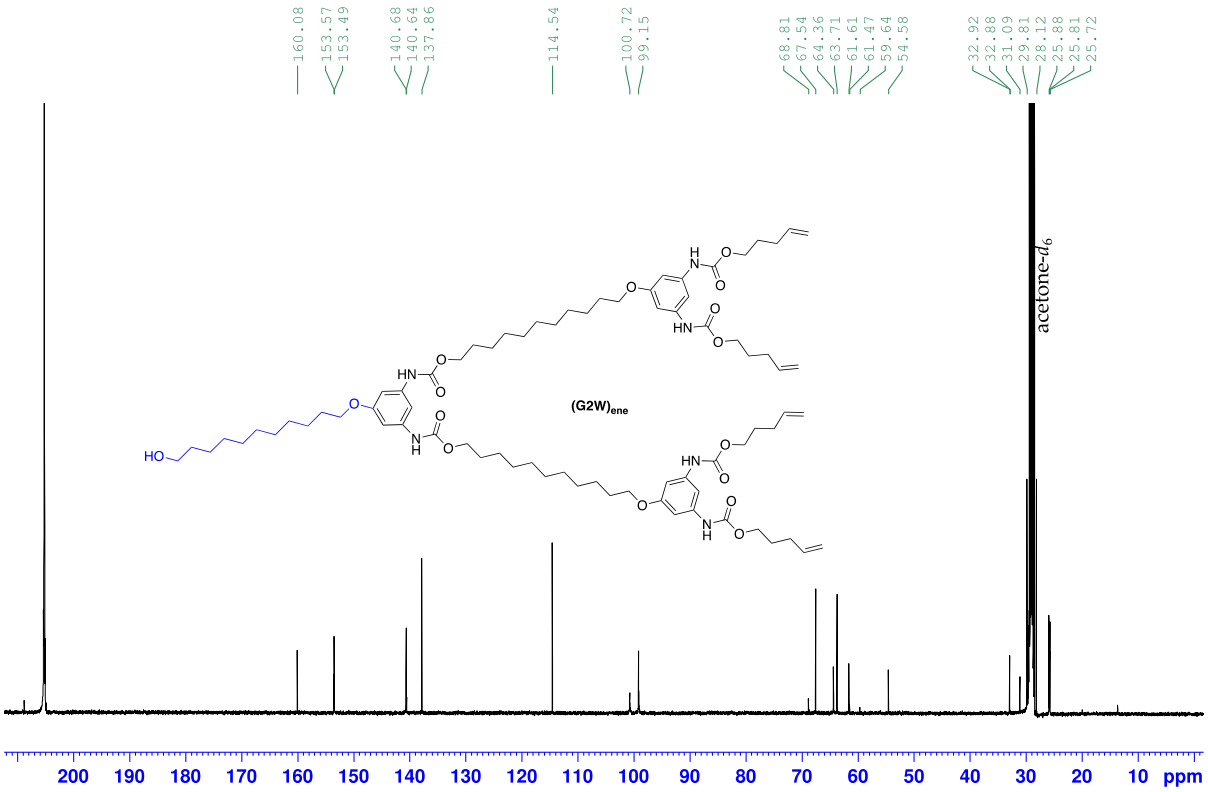

Figure S13. ^{13}C NMR spectrum (126 MHz, CD_3COCD_3, 298 K) of **(G2W)$_{ene}$**.

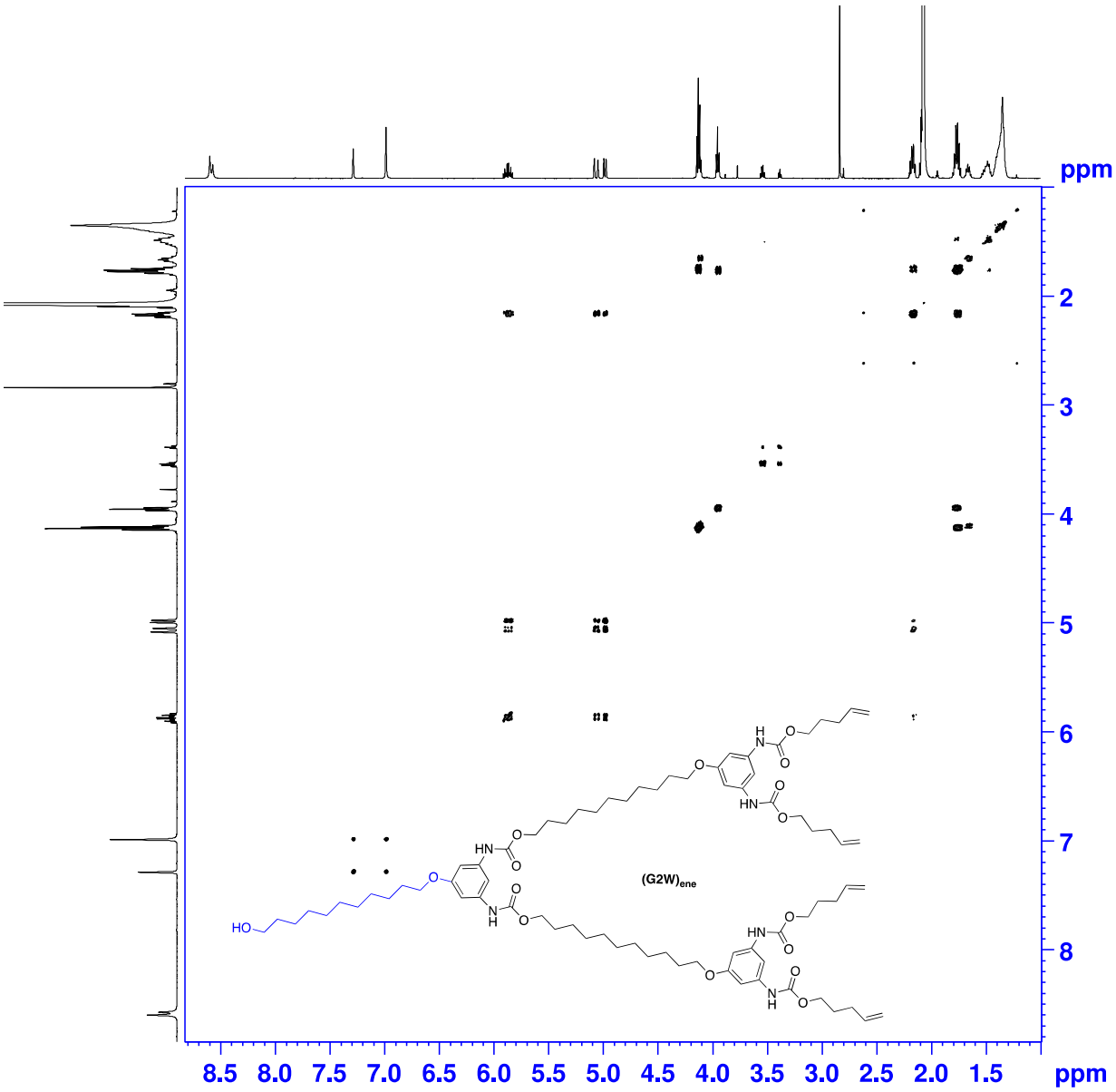

Figure S14. COSY (^{1}H-^{1}H) spectrum (500 MHz, CD_3COCD_3, 298 K) of **(G2W)$_{ene}$**.

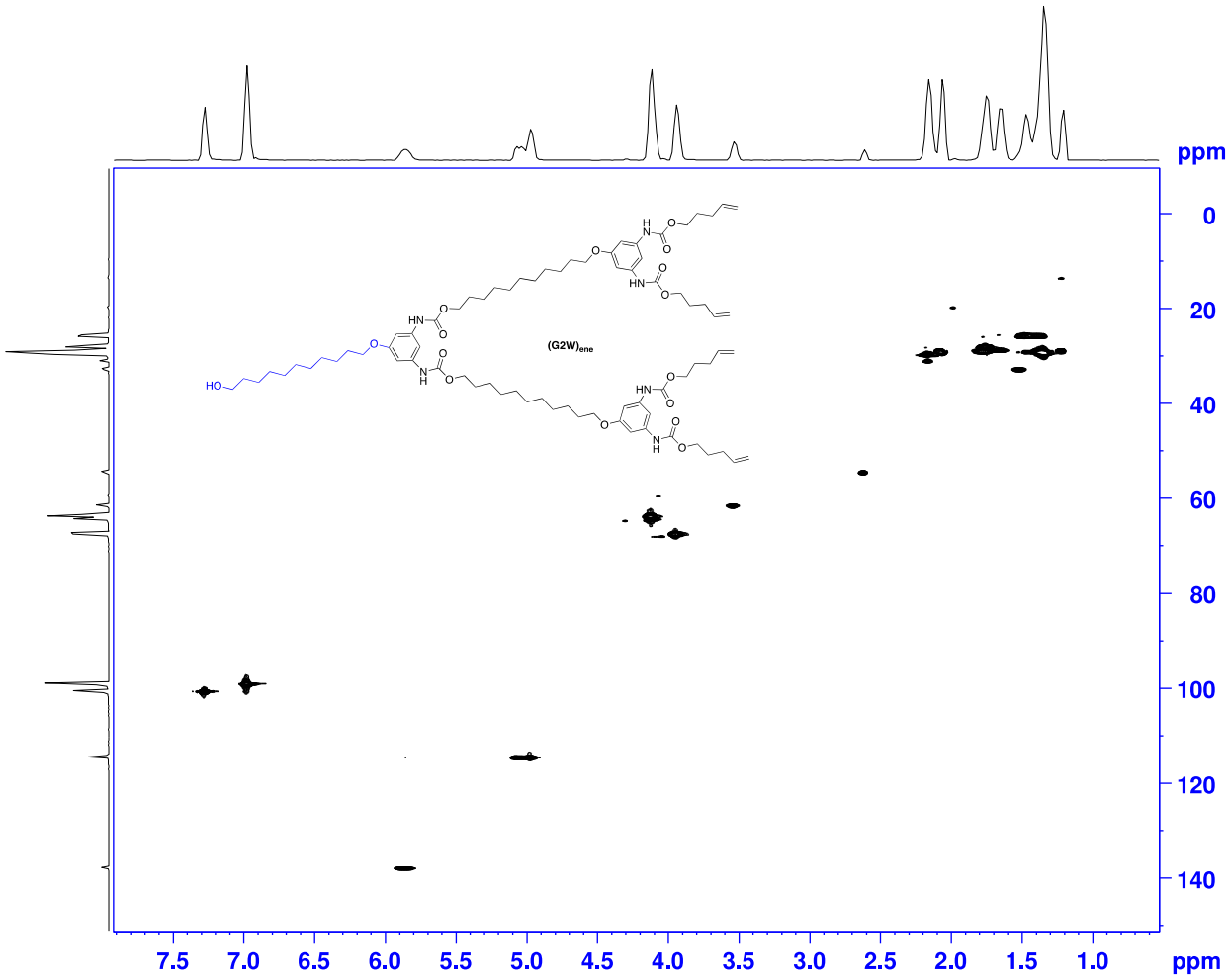

Figure S15. HSQC (^{1}H-^{13}C) spectrum (500 MHz, CD_3COCD_3, 298 K) of **$(G2W)_{ene}$**.

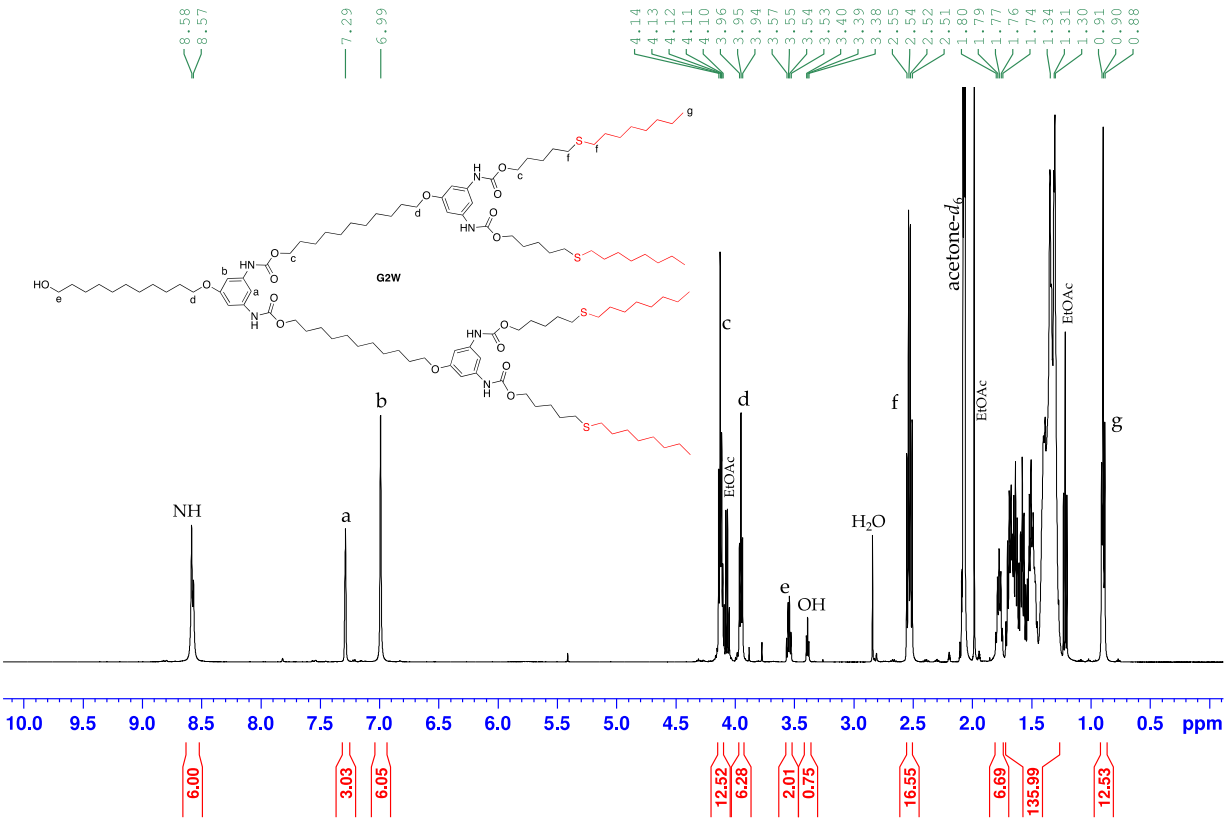

Figure S16. ^{1}H NMR spectrum (500 MHz, CD_3COCD_3, 298 K) of **G2W**.

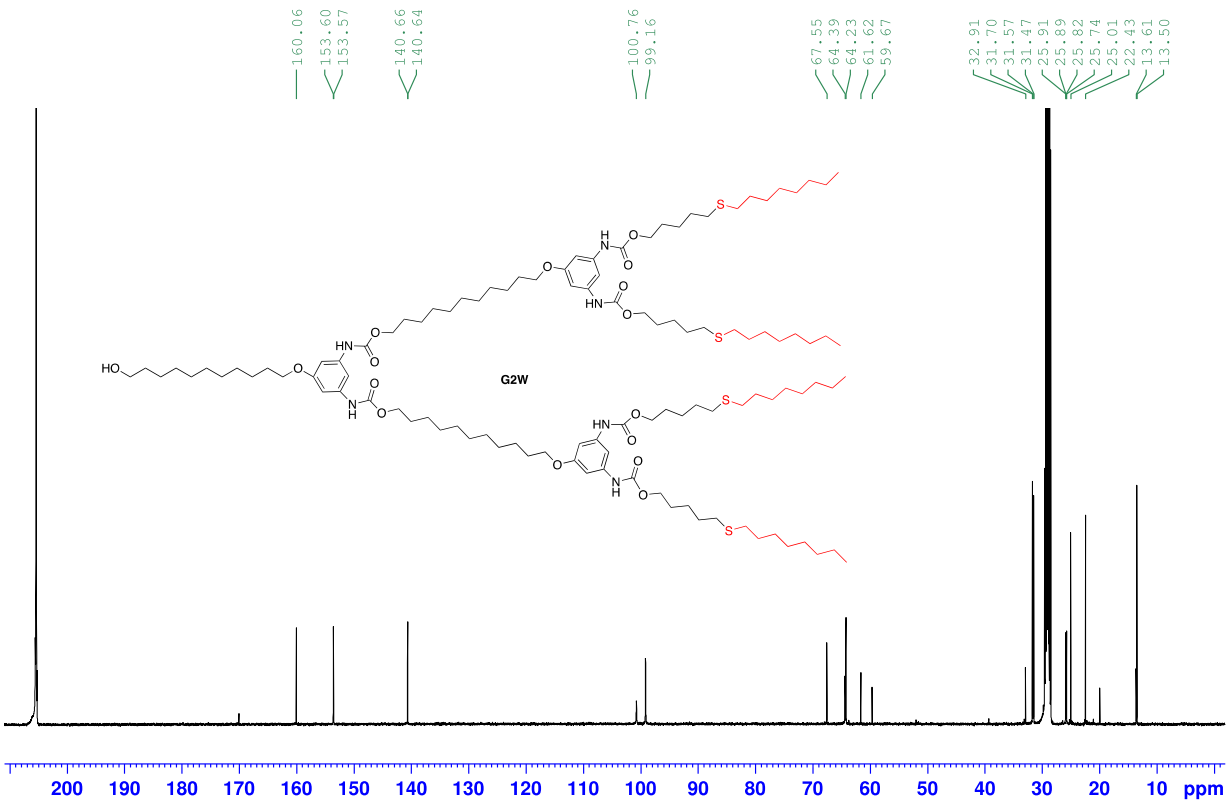

Figure S17. ^{13}C NMR spectrum (126 MHz, CD_3COCD_3, 298 K) of **G2W**.

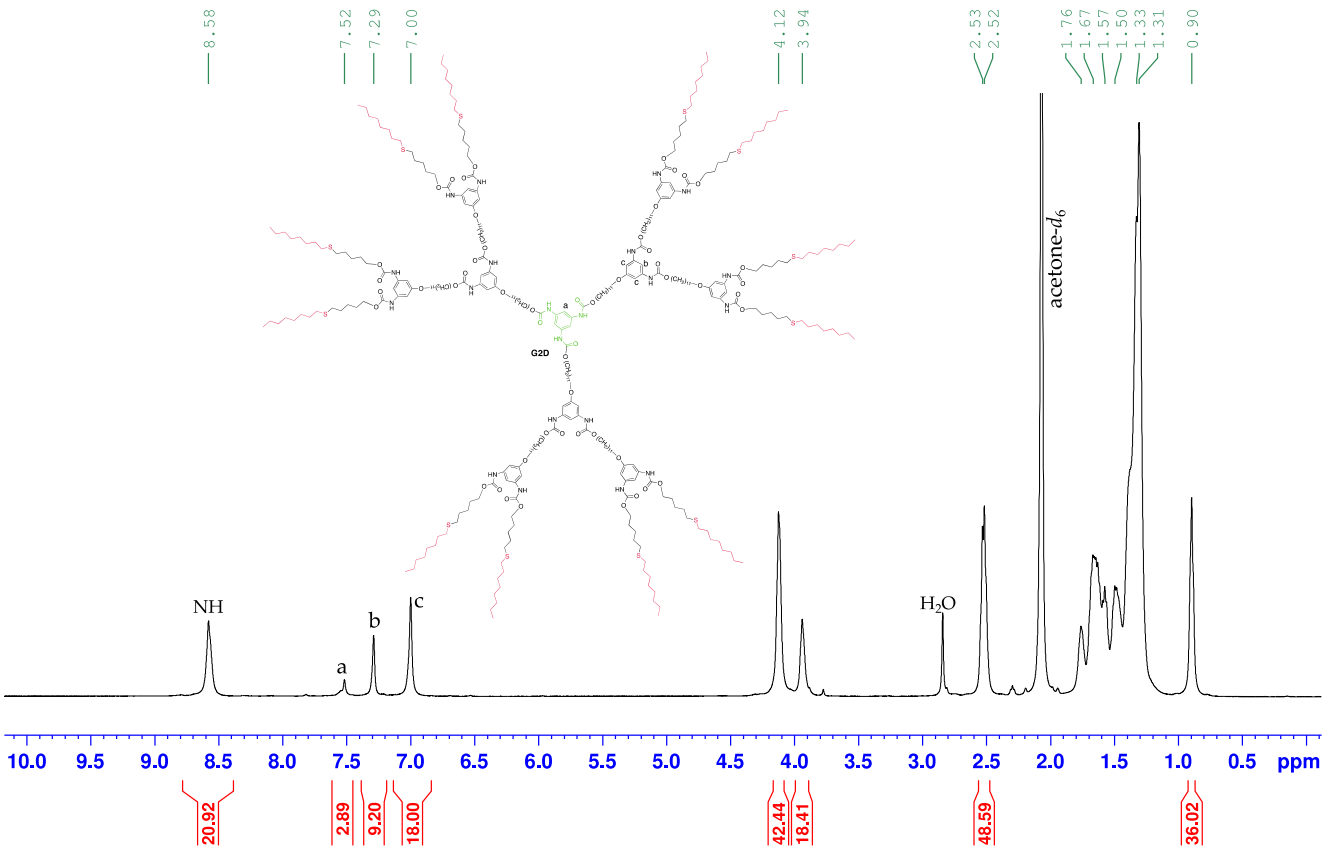

Figure S18. ^{1}H NMR spectrum (500 MHz, CD_3COCD_3, 298 K) of **G2D**.

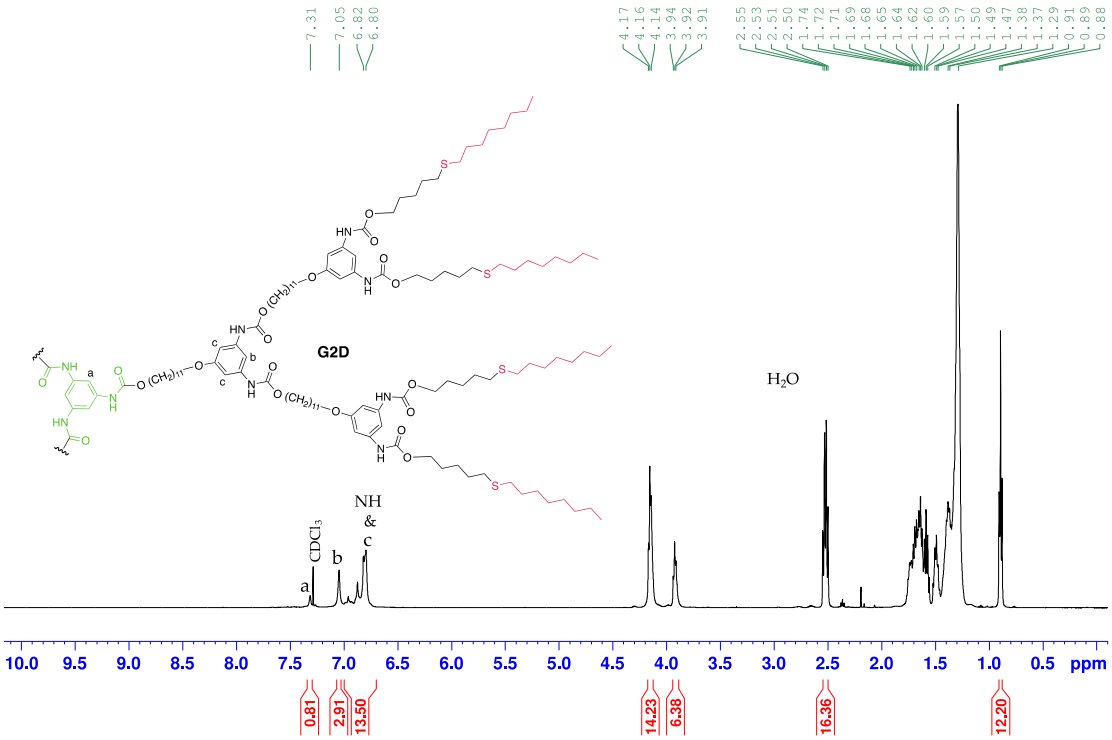

Figure S19. ^{1}H NMR spectrum (500 MHz, $CDCl_3$, 298 K) of **G2D**.

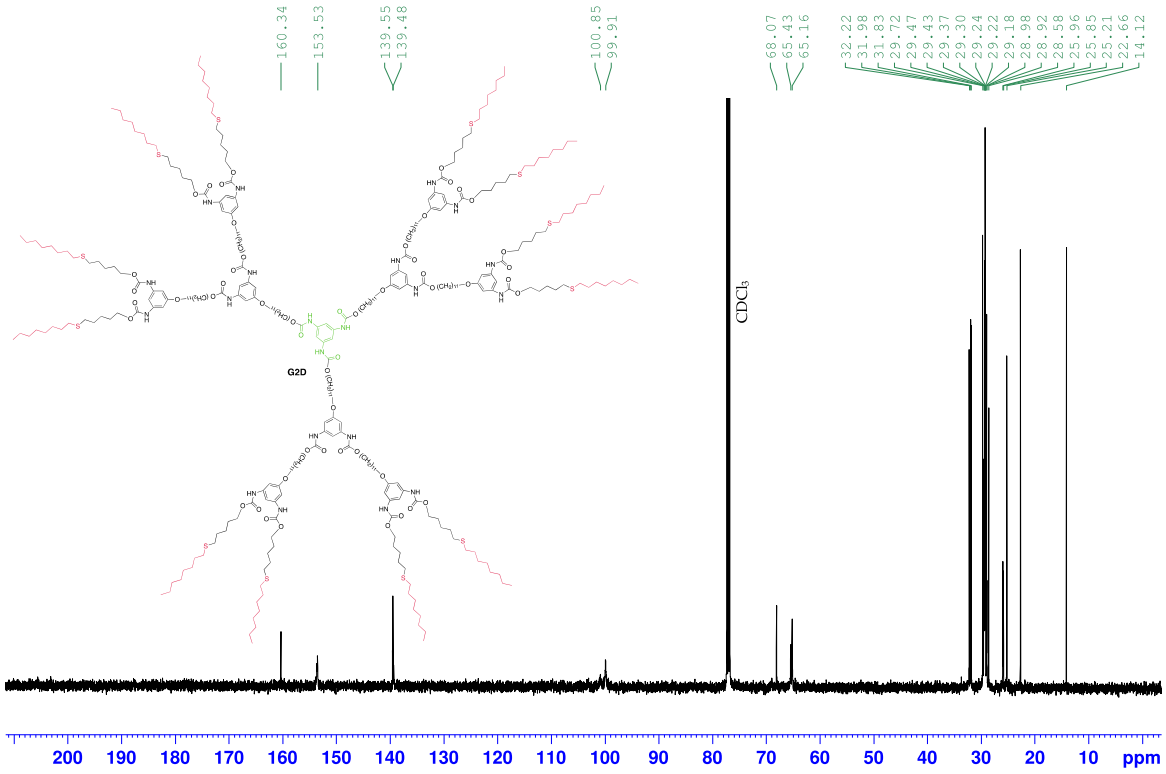

Figure S20. ^{13}C NMR spectrum (126 MHz, $CDCl_3$, 298 K) of **G2D**.

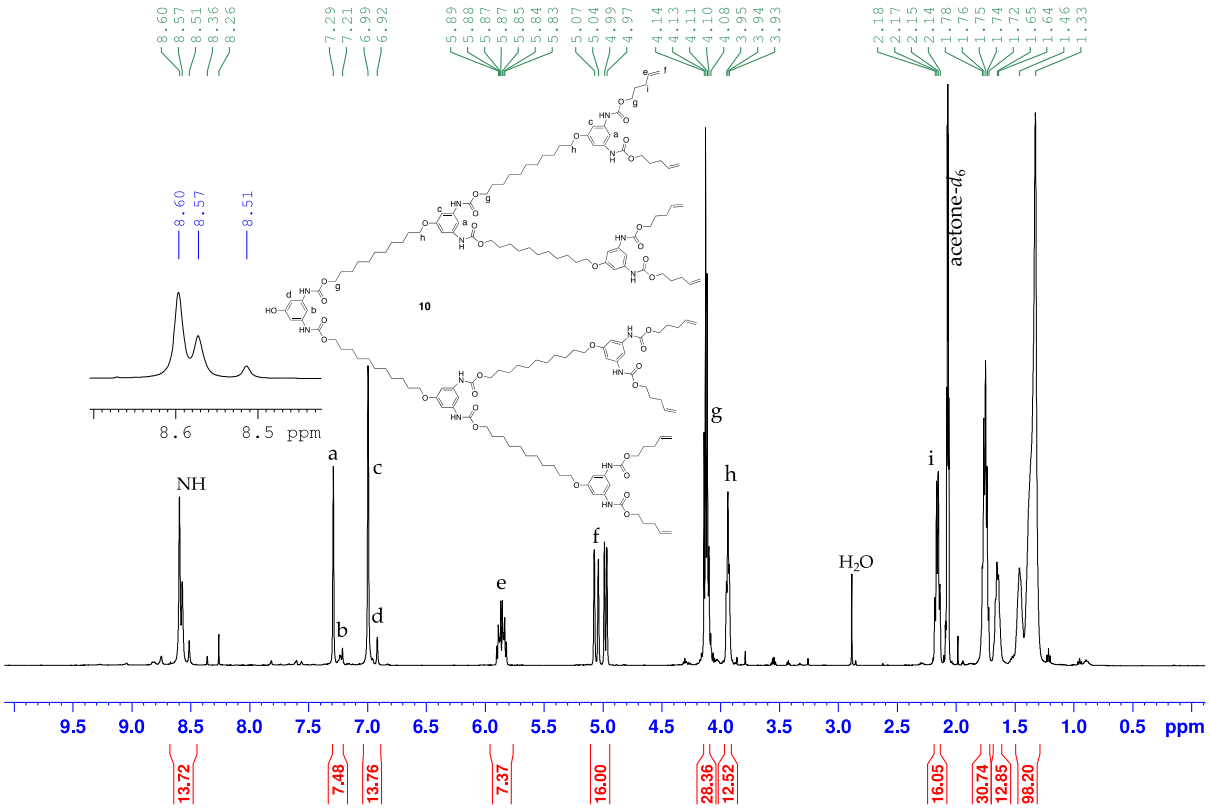

Figure S21. ^{1}H NMR spectrum (500 MHz, CD_3COCD_3, 298 K) of G3 phenolic wedge **10**.

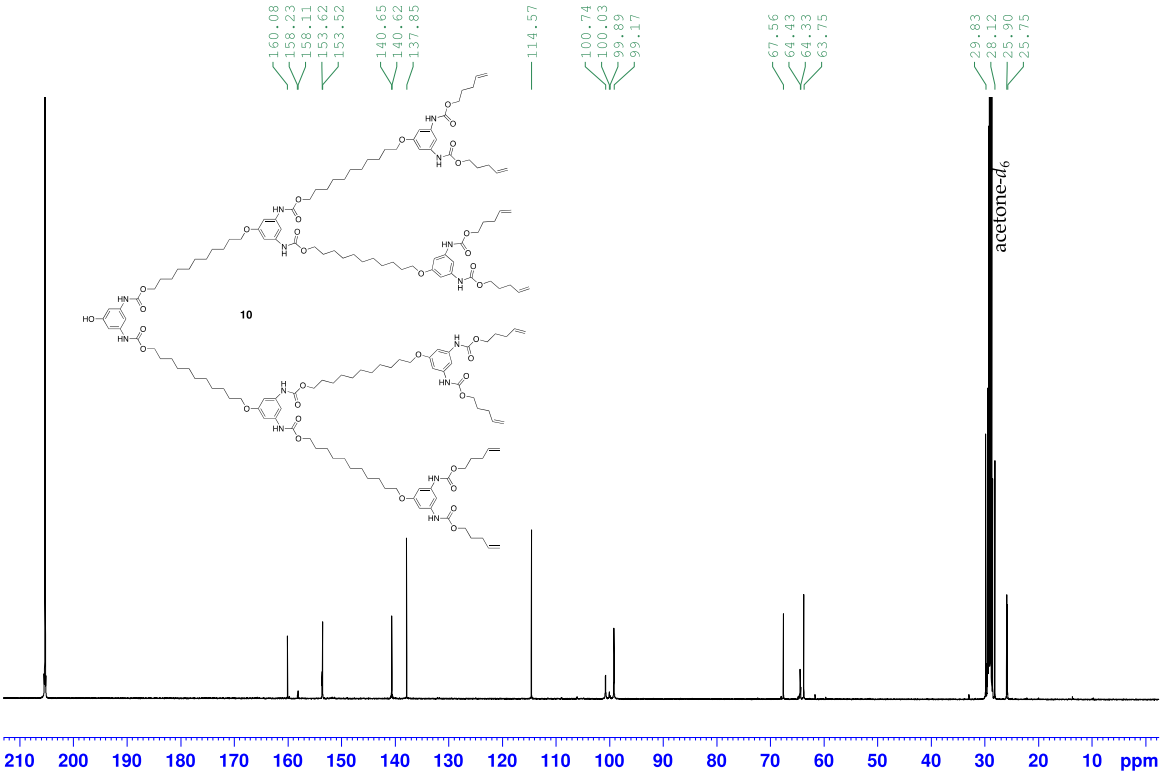

Figure S22. ^{13}C NMR spectrum (126 MHz, CD_3COCD_3, 298 K) of G3 phenolic wedge **10**.

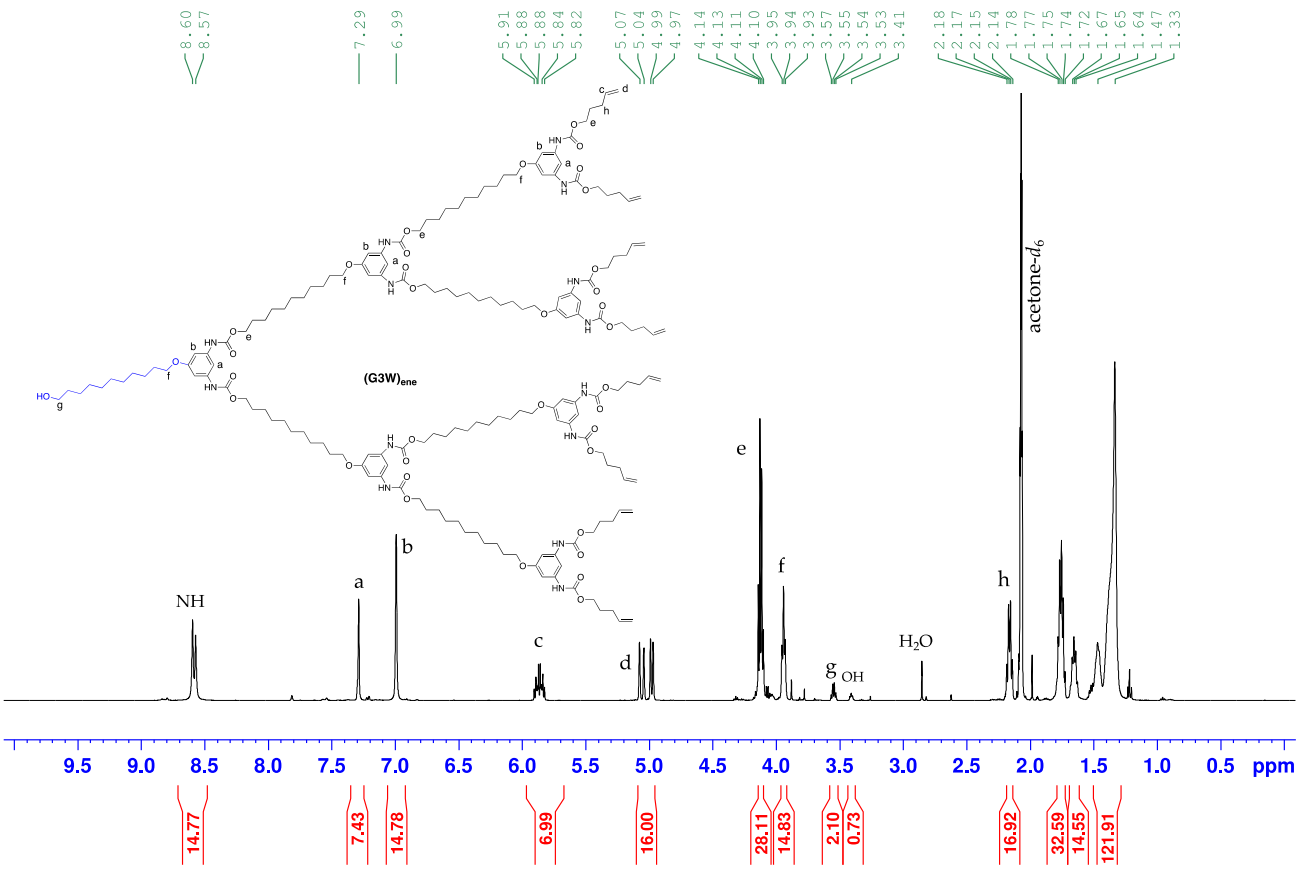

Figure S23. ^{1}H NMR spectrum (500 MHz, CD_3COCD_3, 298 K) of **$(G3W)_{ene}$**.

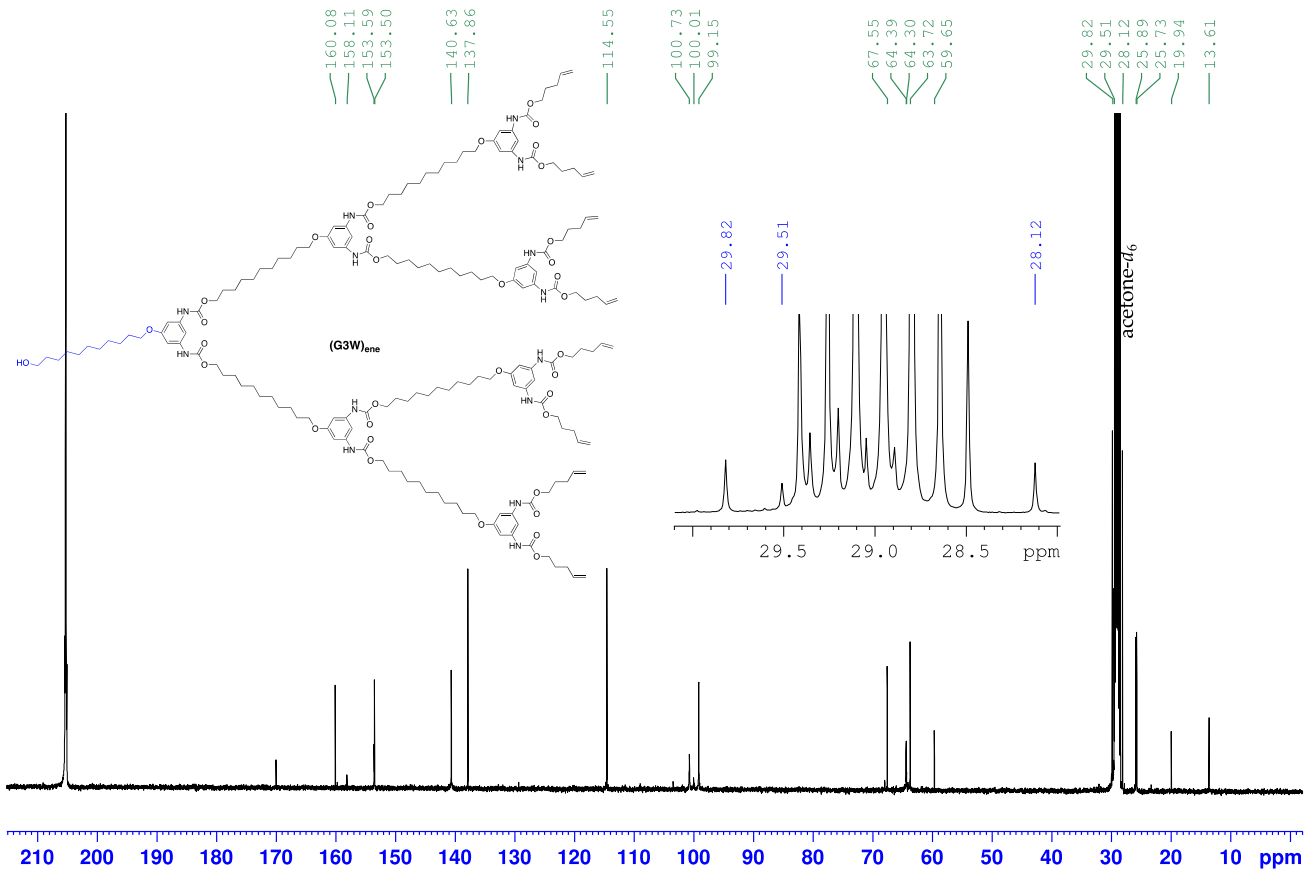

Figure S24. ^{13}C NMR spectrum (126 MHz, CD_3COCD_3, 298 K) of **(G3W)$_{ene}$**.

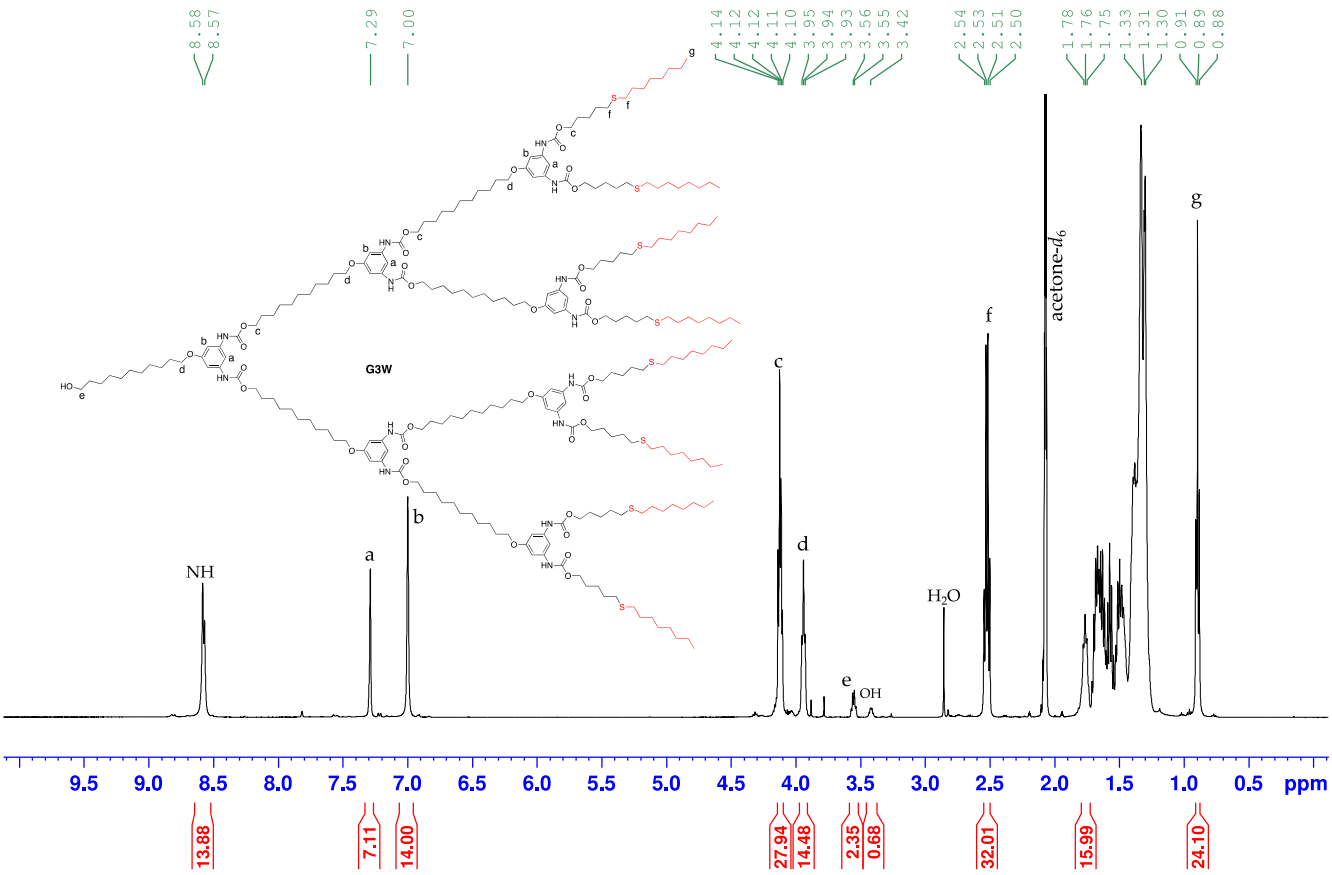

Figure S25. ^{1}H NMR spectrum (500 MHz, CD_3COCD_3, 298 K) of **G3W**.

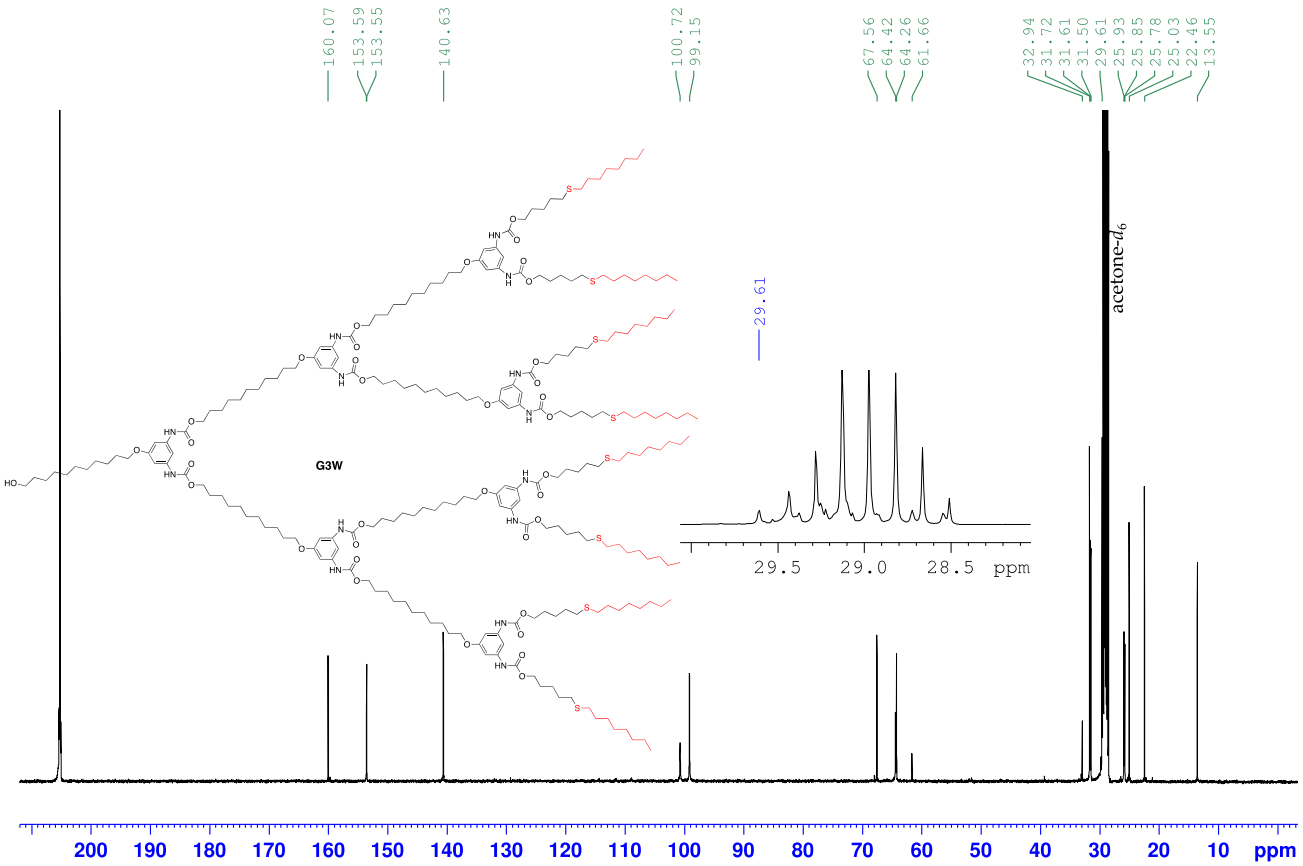

Figure S26. ^{13}C NMR spectrum (126 MHz, CD_3COCD_3, 298 K) of **G3W**.

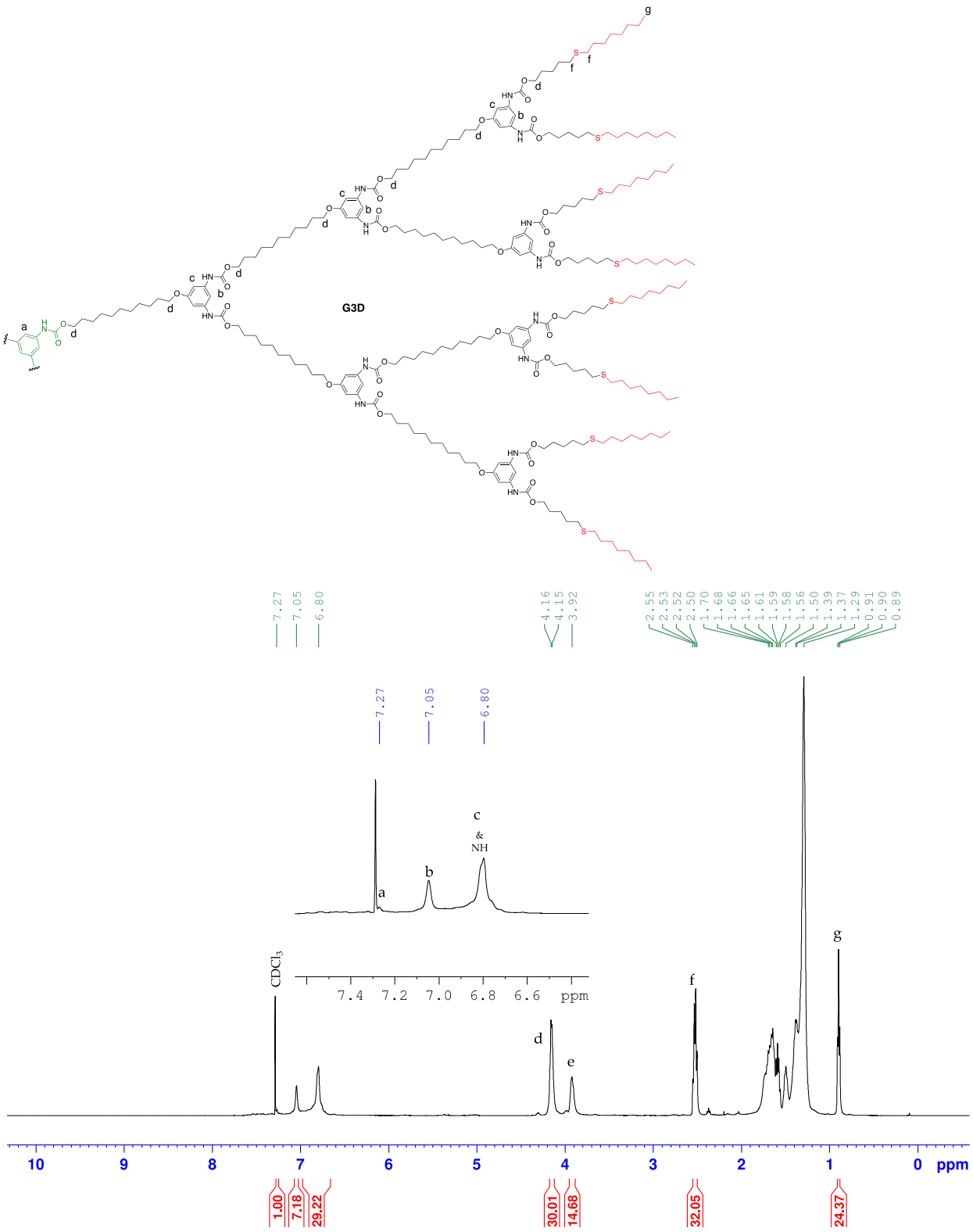

Figure S27. ^{1}H NMR spectrum (500 MHz, $CDCl_3$, 298 K) of **G3D**. The aromatic region is expanded (*at the top*).

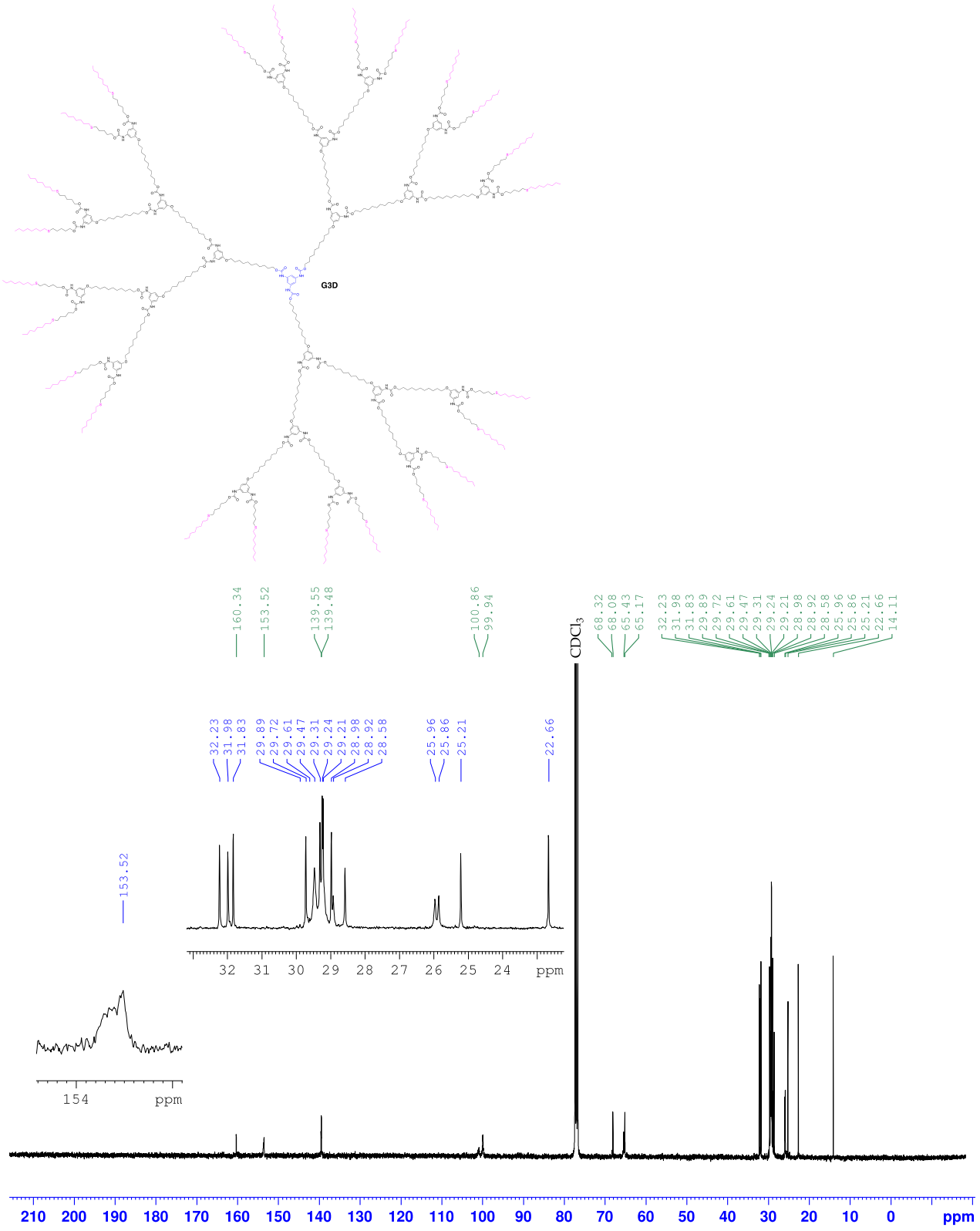

Figure S28. ^{13}C NMR spectrum (126 MHz, $CDCl_3$, 298 K) of **G3D**.

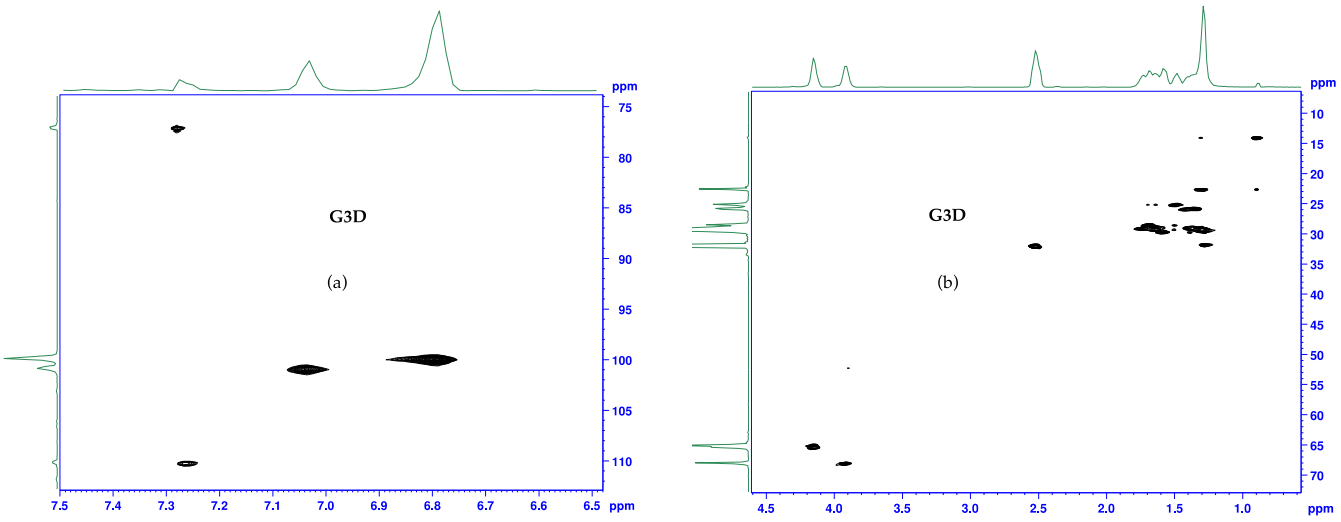

Figure S29. HSQC (^{1}H-^{13}C) spectrum (500 MHz, $CDCl_3$, 298 K) of **G3D** showing (a) the aromatic and (b) the aliphatic region.

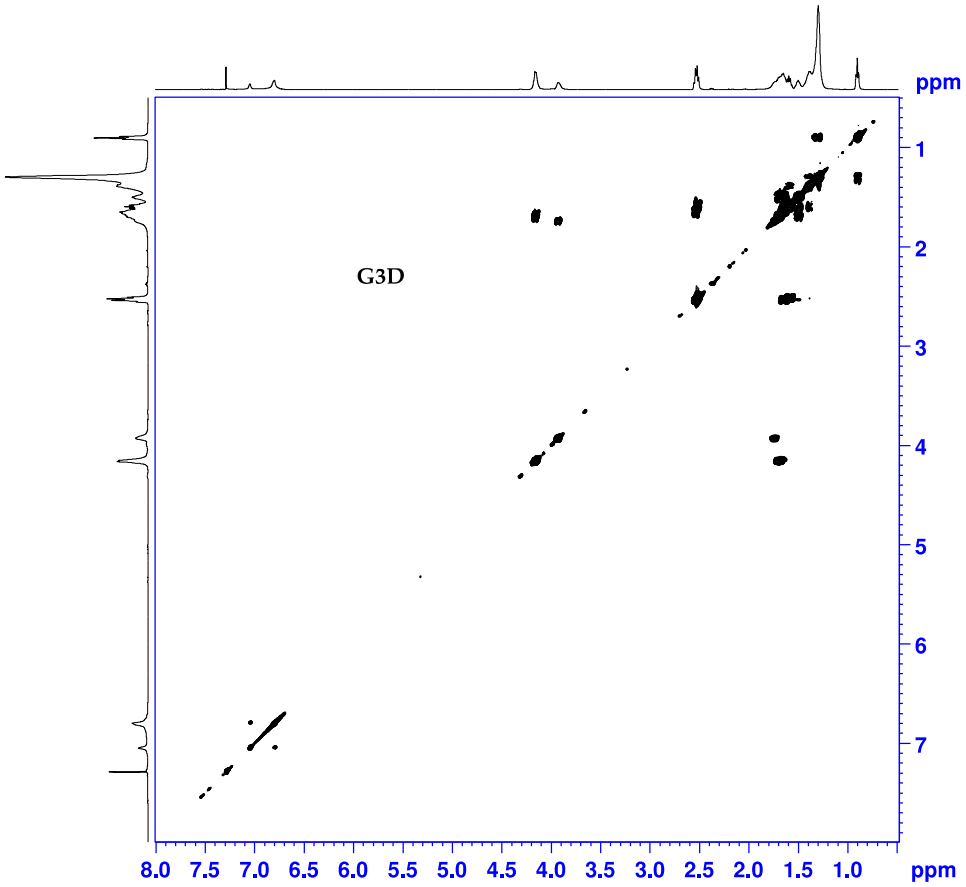

Figure S30. COSY (^{1}H-^{1}H) spectrum (500 MHz, $CDCl_3$, 298 K) of **G3D**.

3. 2D-Diffusion order experiment (DOSY) (of G1 – G3 dendrimers

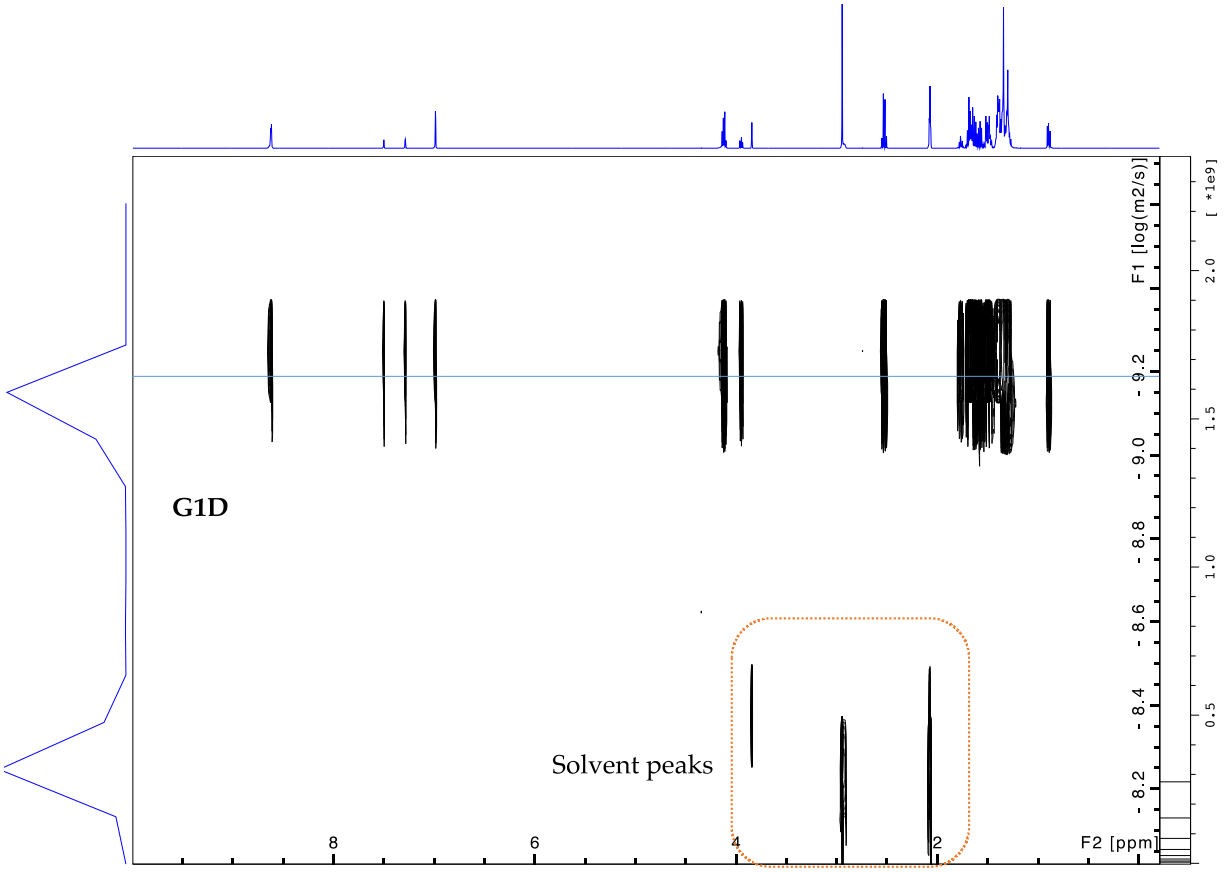

Figure S31. 2-D DOSY spectrum (CD_3COCD_3, 298 K, 500 MHz) of the surface functionalized generation-one dendrimer **G1D**, the diffusion coefficient D = 4.47 x 10^{-10} m^2/s.

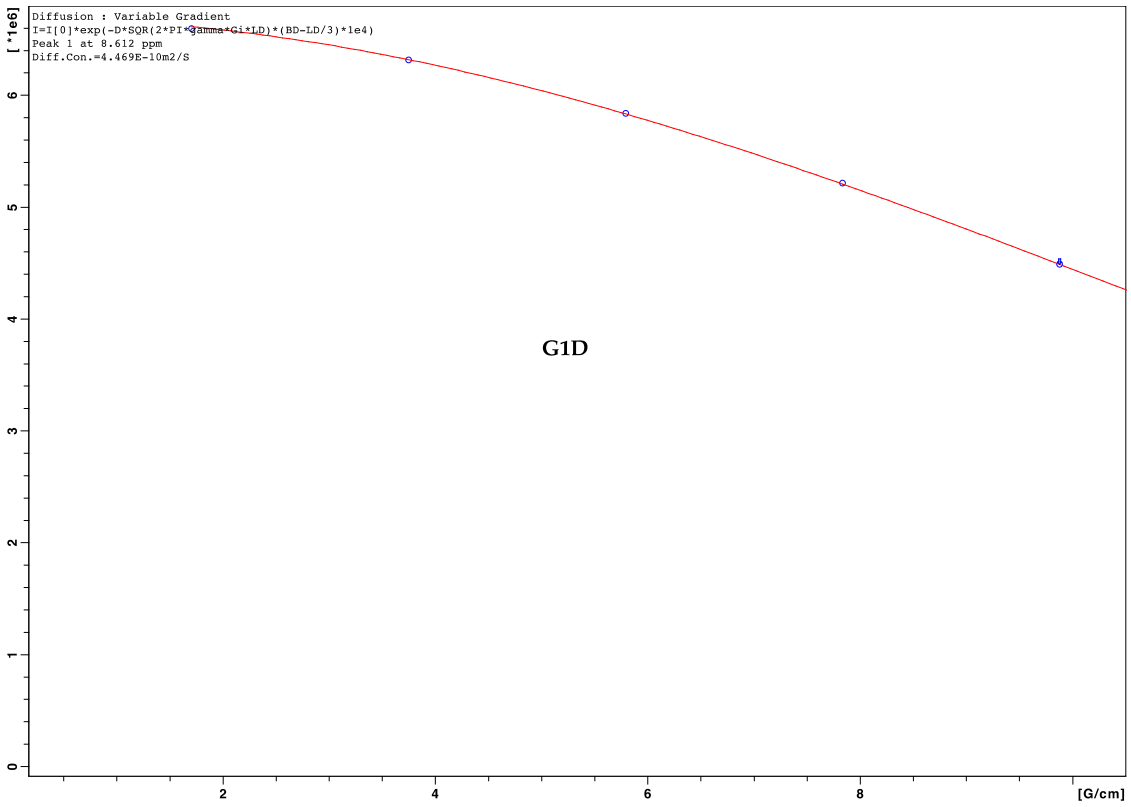

Figure S32. Showing fitting function after fitting with *SimFit (T1/T2)* analysis. The fitting curve for the peak at 8.612 ppm of **G1D** (CD_3COCD_3, 298 K, 500 MHz) is shown.

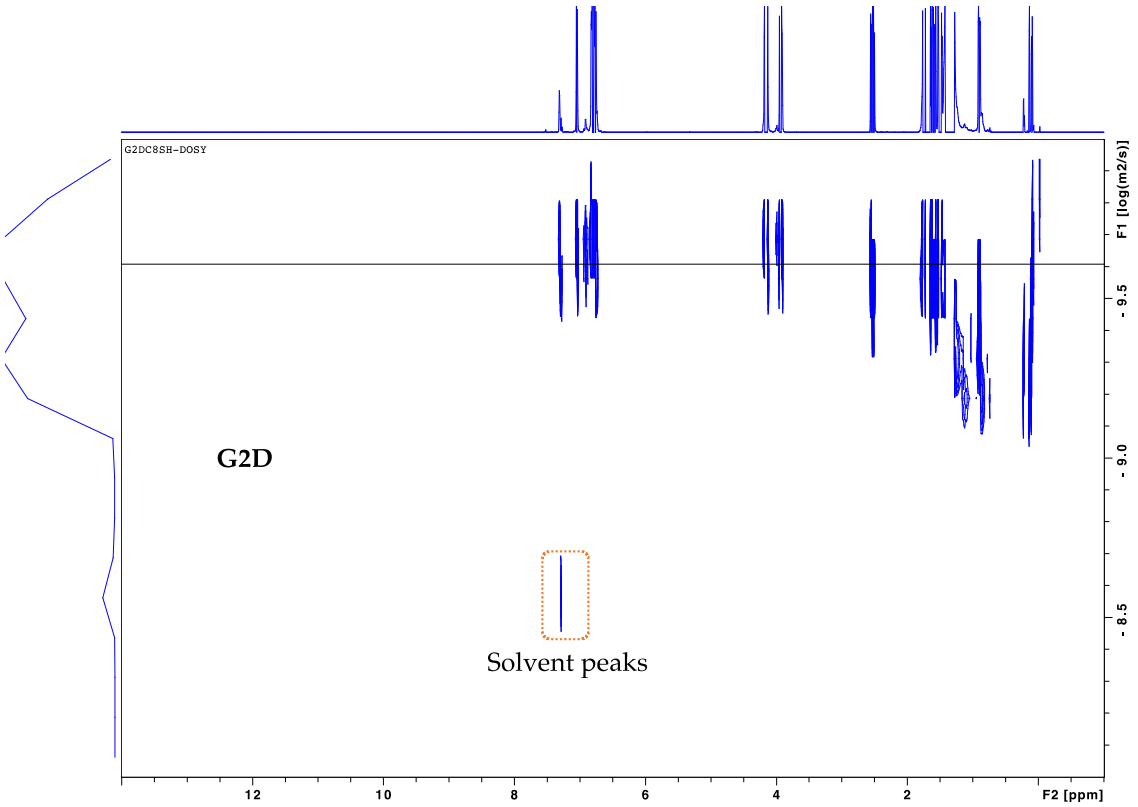

Figure S33. 2-D DOSY spectrum ($CDCl_3$, 298 K, 500 MHz) of the surface functionalized generation-two dendrimer **G2D**, the diffusion coefficient D = 1.857 x 10^{-10} m^2/s.

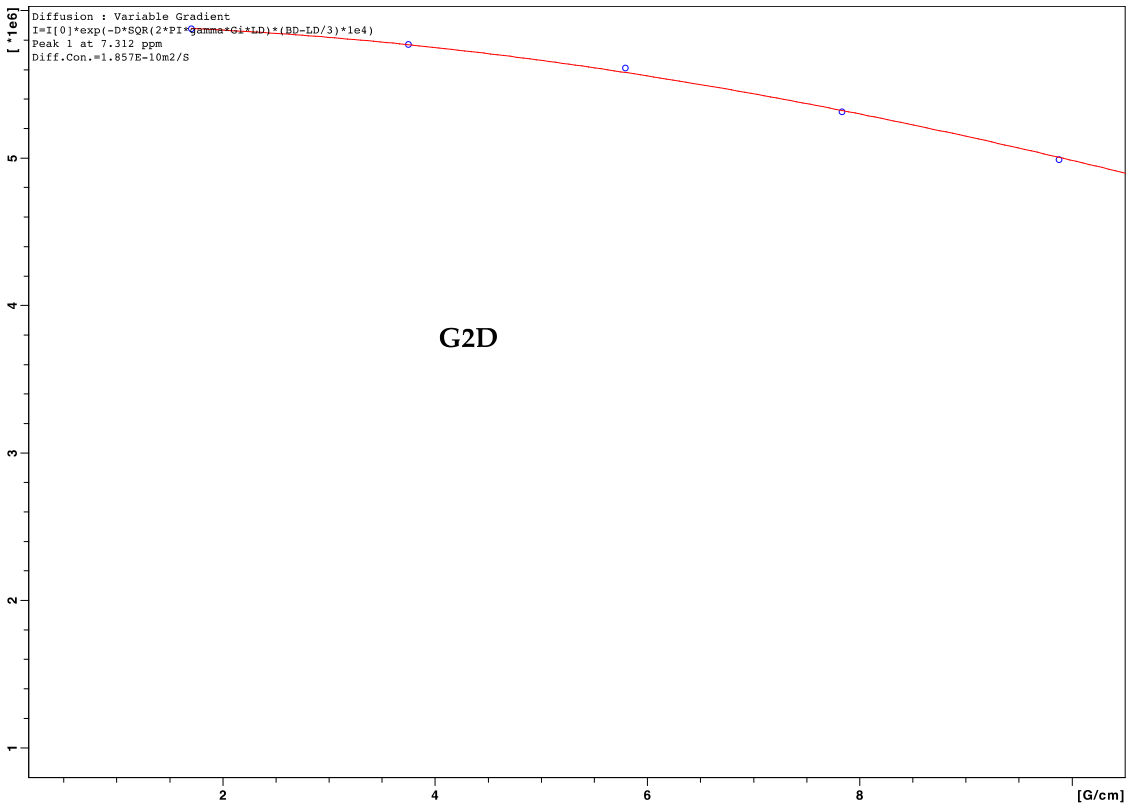

Figure S34. Showing fitting function after fitting with *SimFit (T1/T2)* analysis. The fitting curve for the peak at 7.312 ppm of **G2D** ($CDCl_3$, 298 K, 500 MHz) is shown.

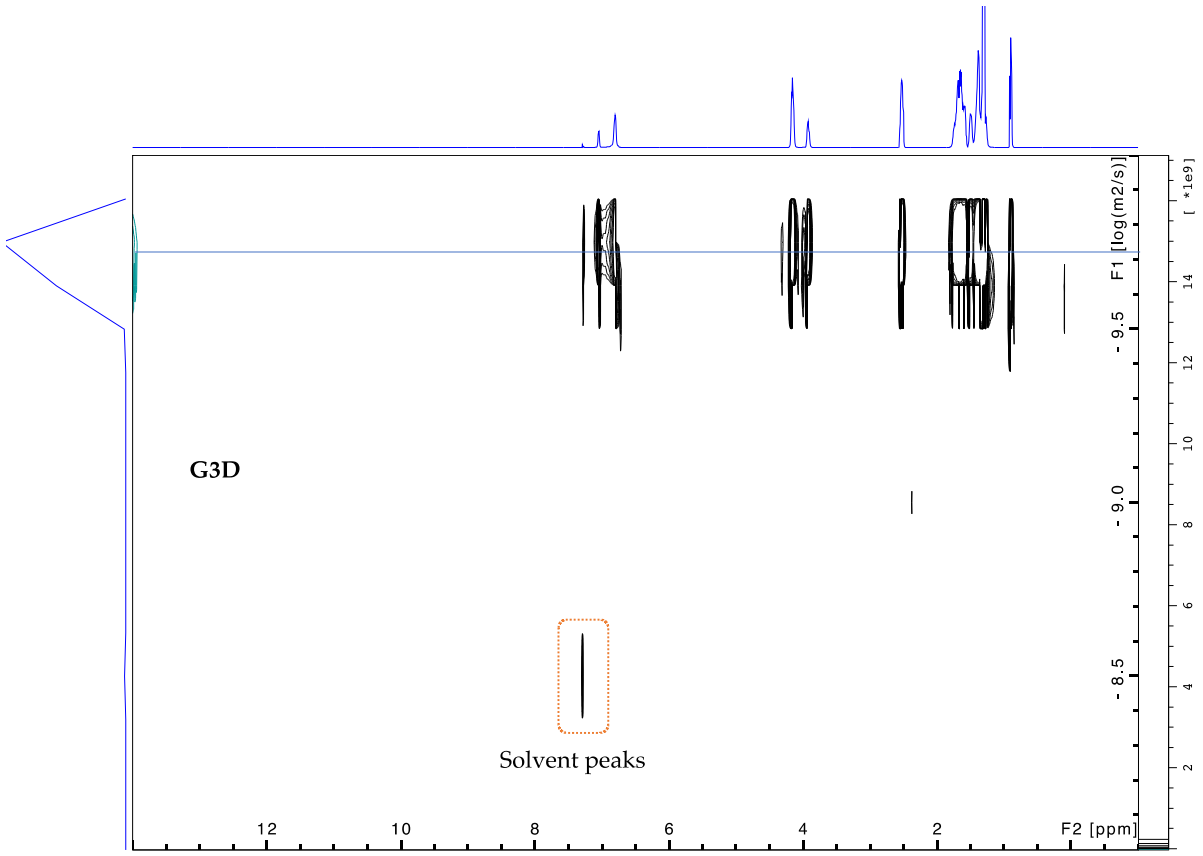

Figure S35. 2-D DOSY spectrum ($CDCl_3$, 298 K, 500 MHz) of the surface functionalized generation-two dendrimer **G3D**, the diffusion coefficient D = 1.381 x 10^{-10} m^2/s.

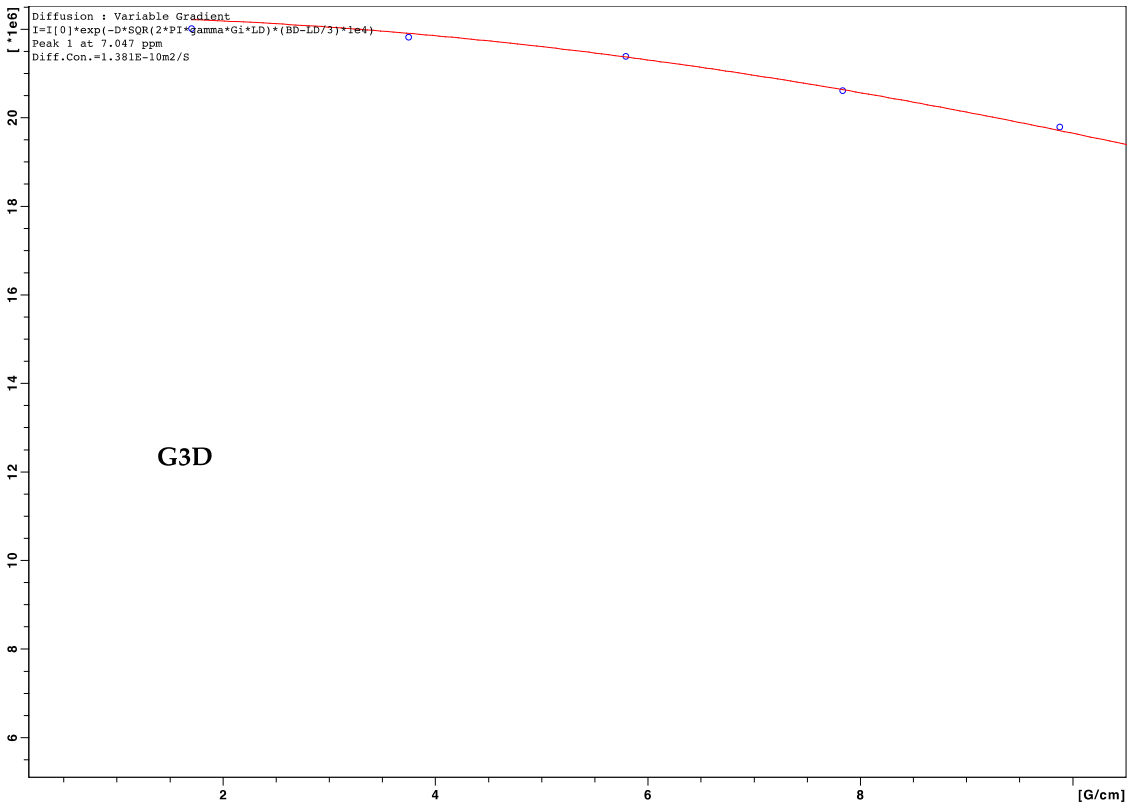

Figure S36. Showing fitting function after fitting with *SimFit (T1/T2)* analysis. The fitting curve for the peak at 7.047 ppm of **G3D** ($CDCl_3$, 298 K, 500 MHz) is shown.

4. Mass spectrometric data of G2 – G3 dendrons and dendrimers.

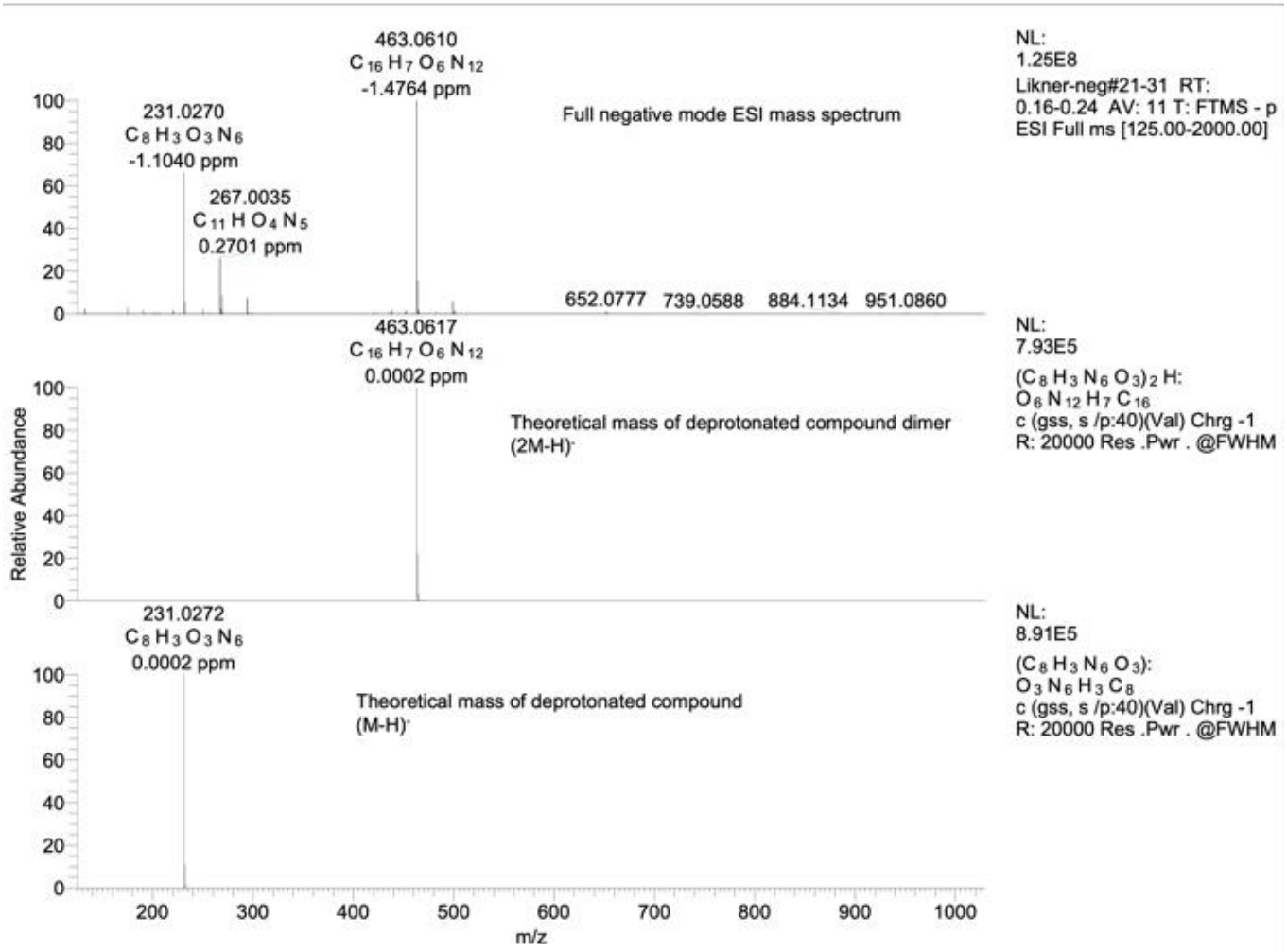

Figure S37. HRMS (ESI-LTQ-Orbitrap) of linking agent **4**.

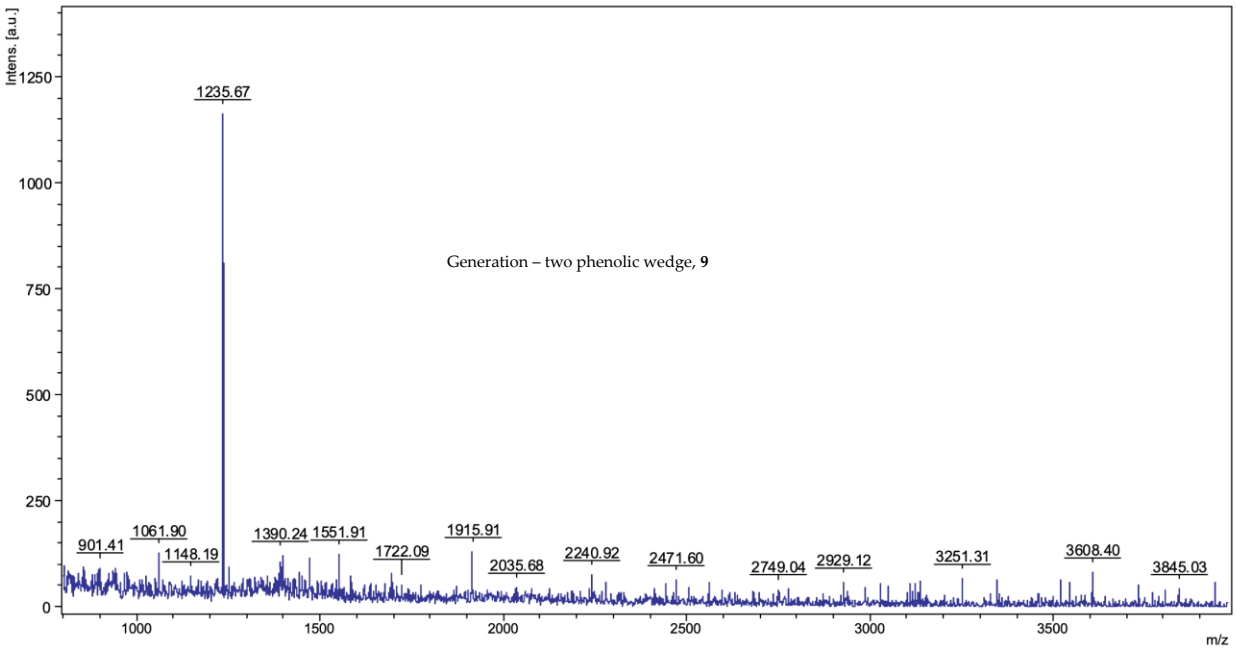

Figure S38. LRMS (MALDI-TOF-MS) of generation – two phenolic wedge **9**.

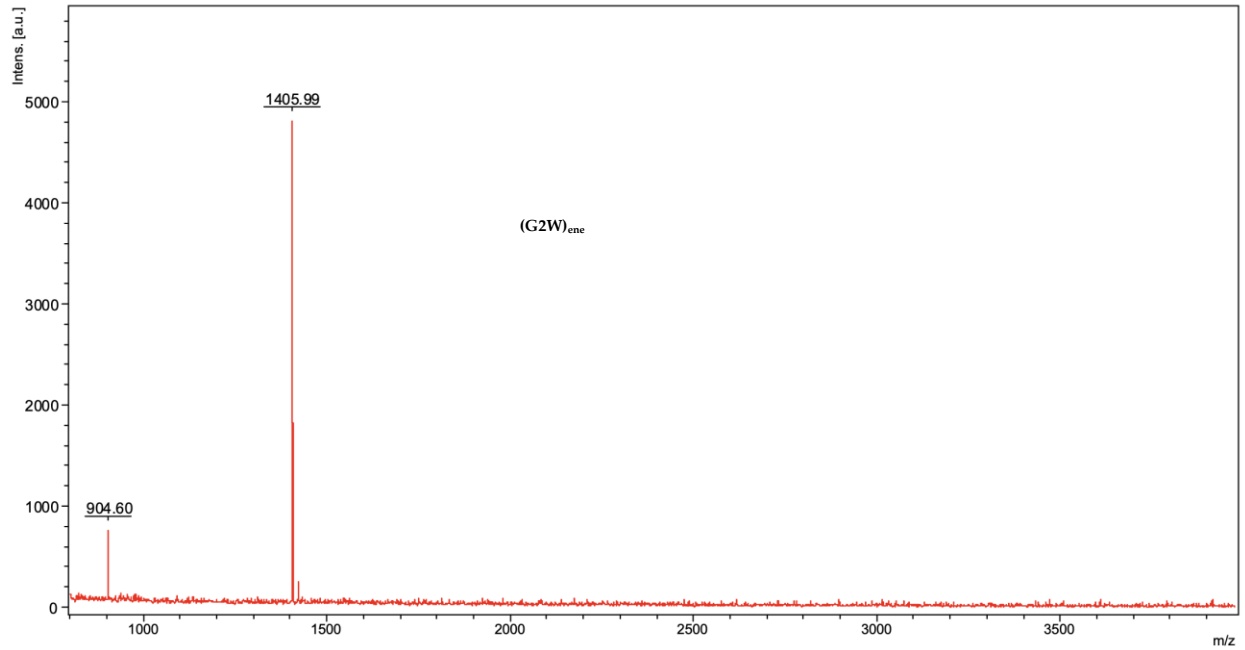

Figure S39. LRMS (MALDI-TOF-MS) of generation – two dendron with alkene periphery, **$(G2W)_{ene}$**.

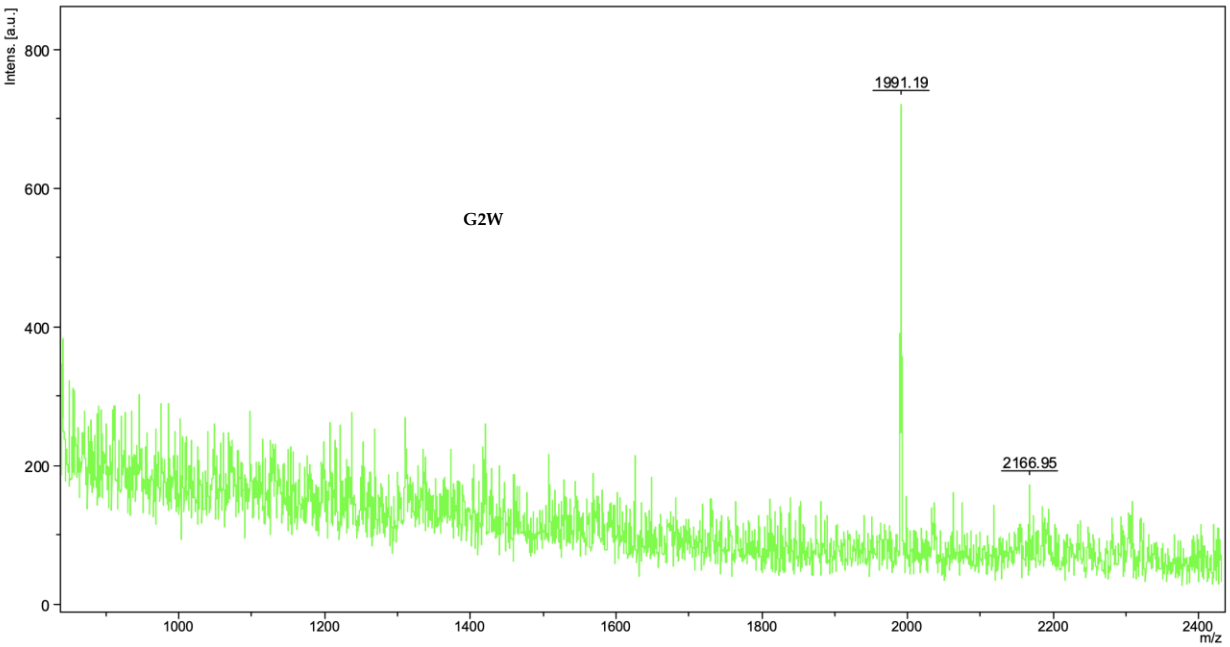

Figure S40. LRMS (MALDI-TOF-MS) of generation – two dendron with alkene periphery, **G2W**.

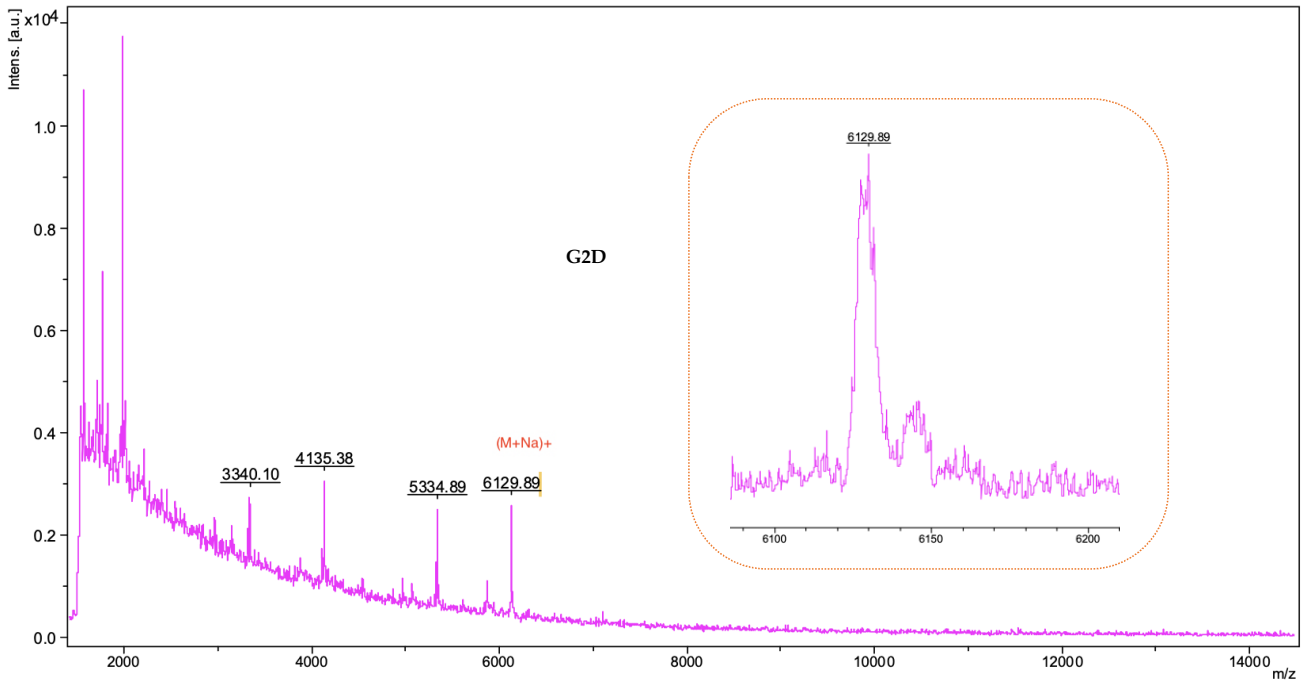

Figure S41. LRMS (MALDI-TOF-MS) of generation – two dendron with alkene periphery, **G2D**.

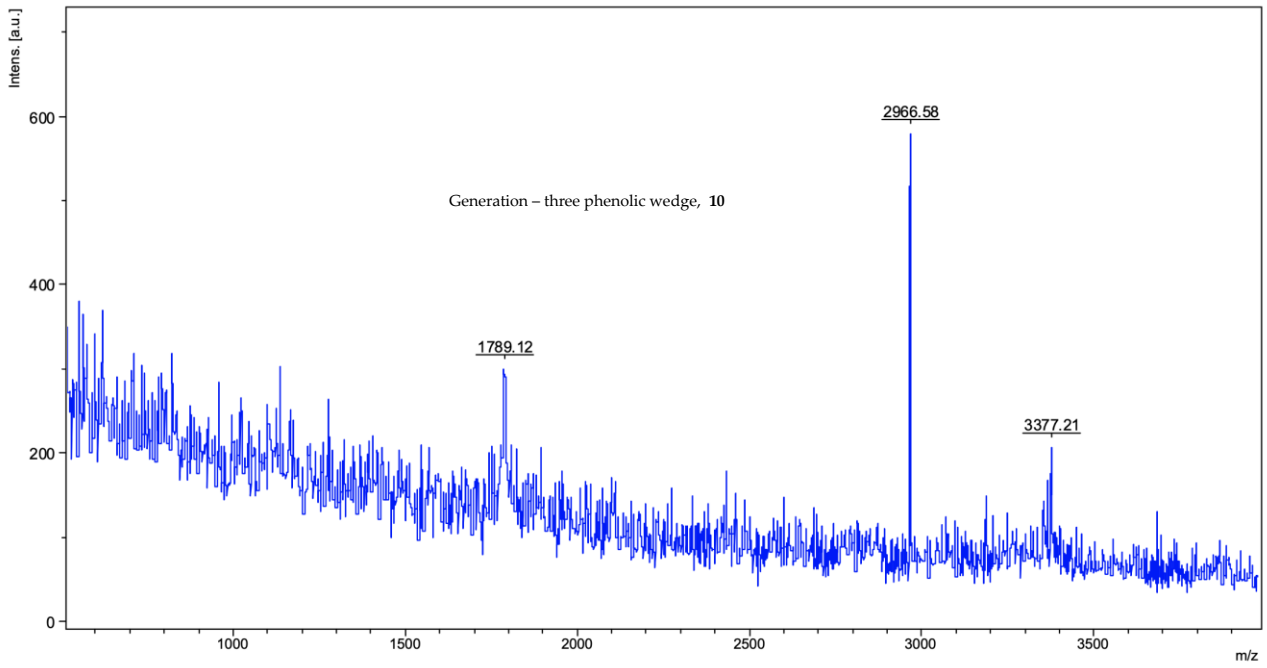

Figure S42. LRMS (MALDI-TOF-MS) of generation – three phenolic wedge **10**.

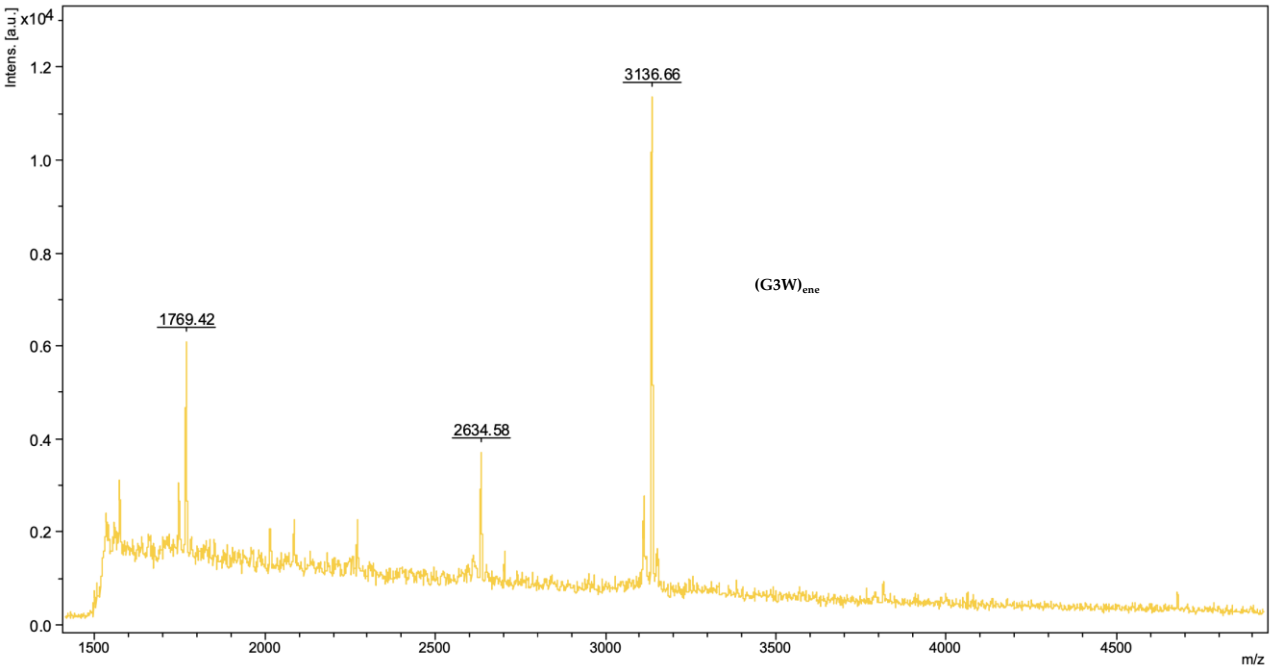

Figure S43. LRMS (MALDI-TOF-MS) of generation – three dendron with alkene periphery, **$(G3W)_{ene}$**.

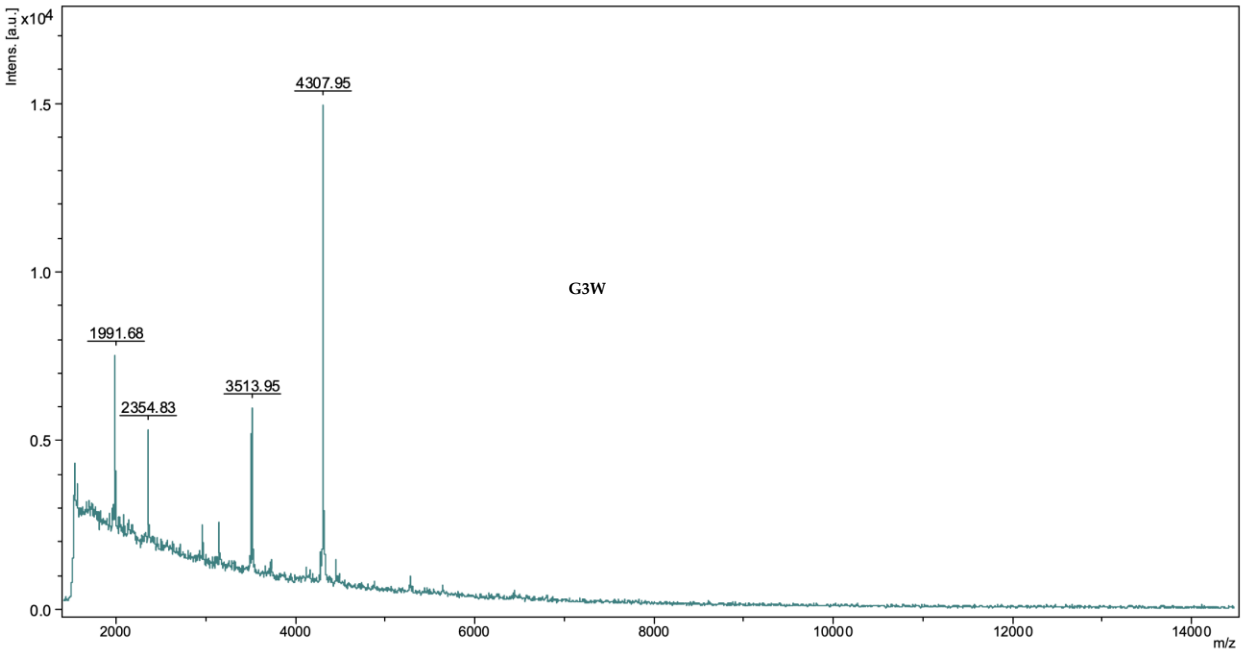

Figure S45. LRMS (MALDI-TOF-MS) of generation-two dendron with alkene periphery, **G3W**.

5. FT – IR spectra of G2 – G3 compounds

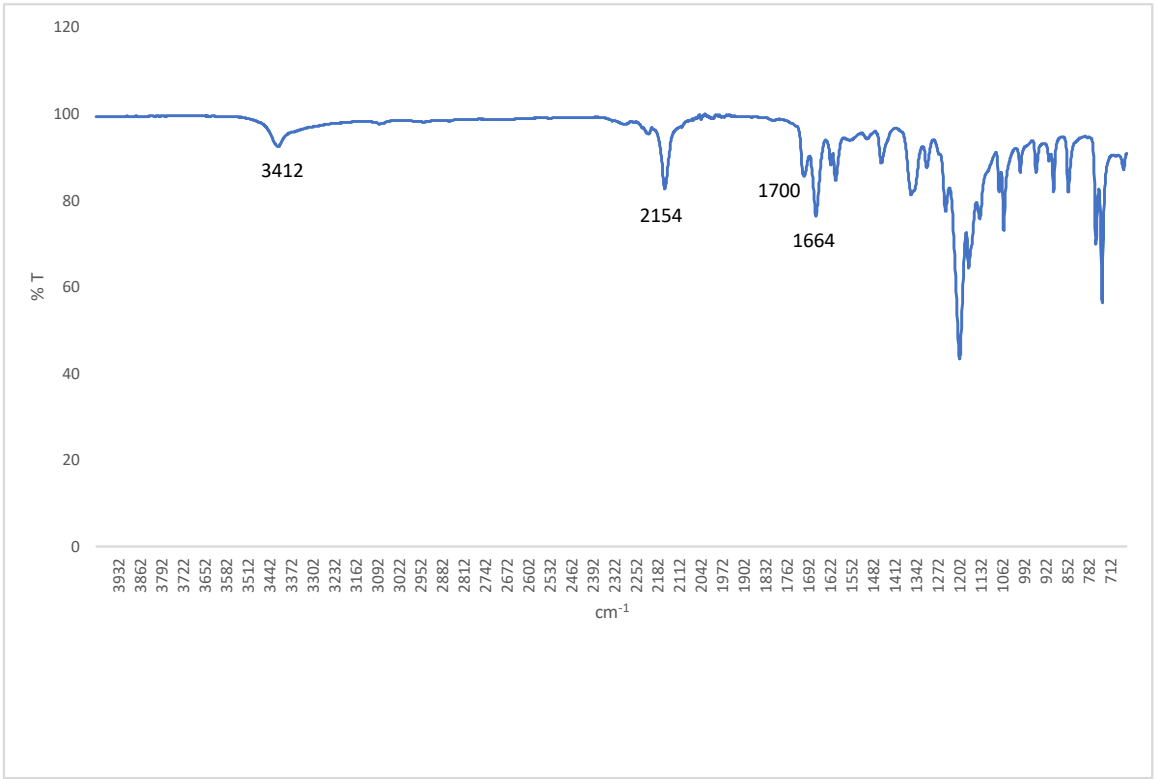

Figure S46. FT-IR spectrum of 5-hydroxy-1,3-benzenedicarbonyl diazide **4**.

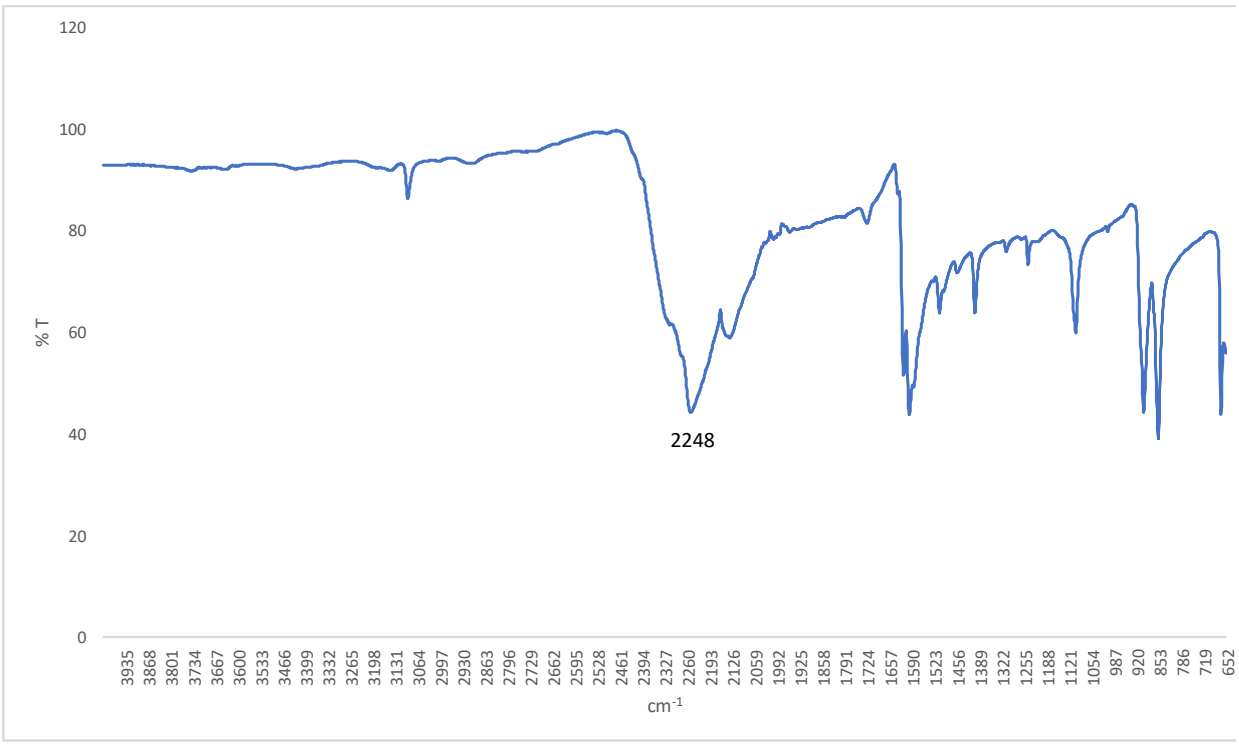

(a)

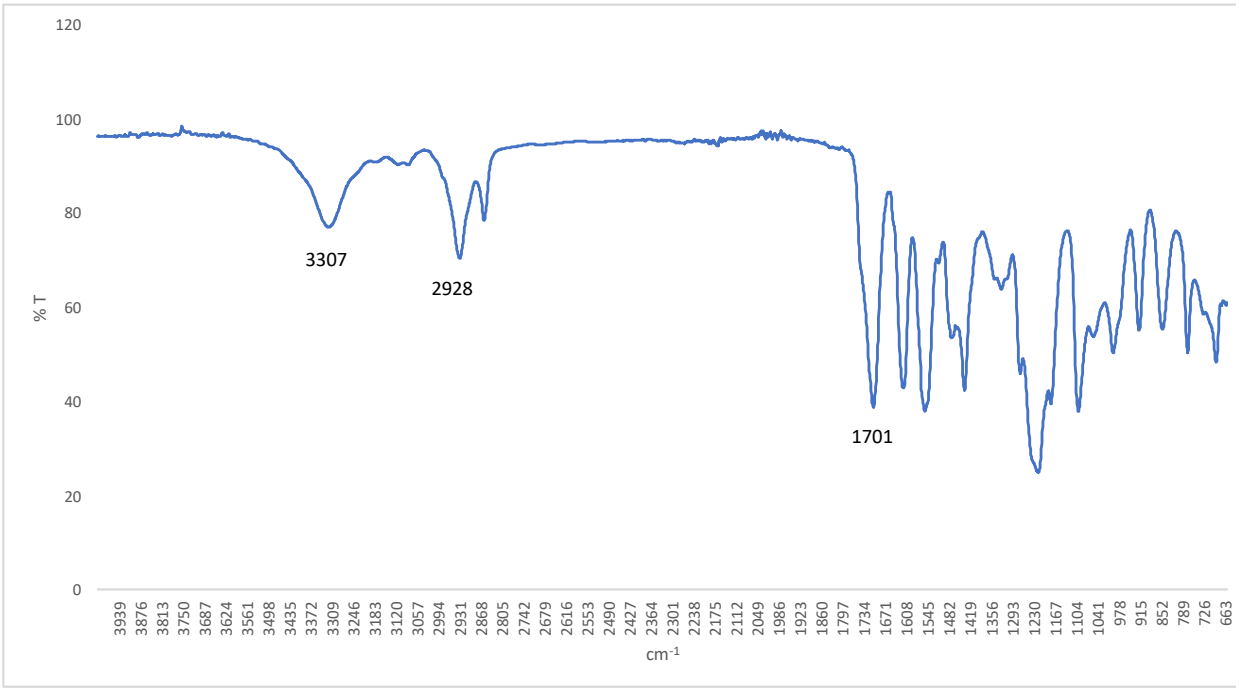

(b)

Figure S47. (**a**) FT-IR spectrum of 1,3,5-triisocyanatobenzene **6**.(**b**) FT-IR spectrum of G2 phenolic wedge **9**.

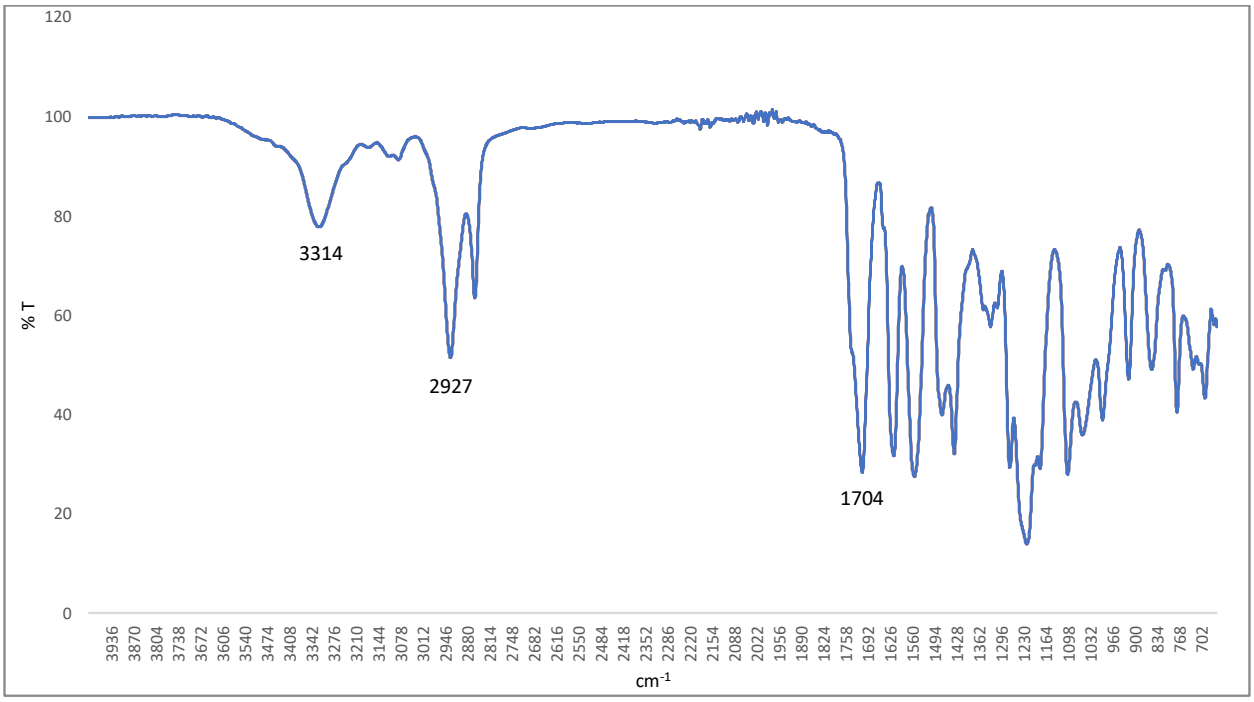

Figure S48. FT-IR spectrum of **$(G2W)_{ene}$**.

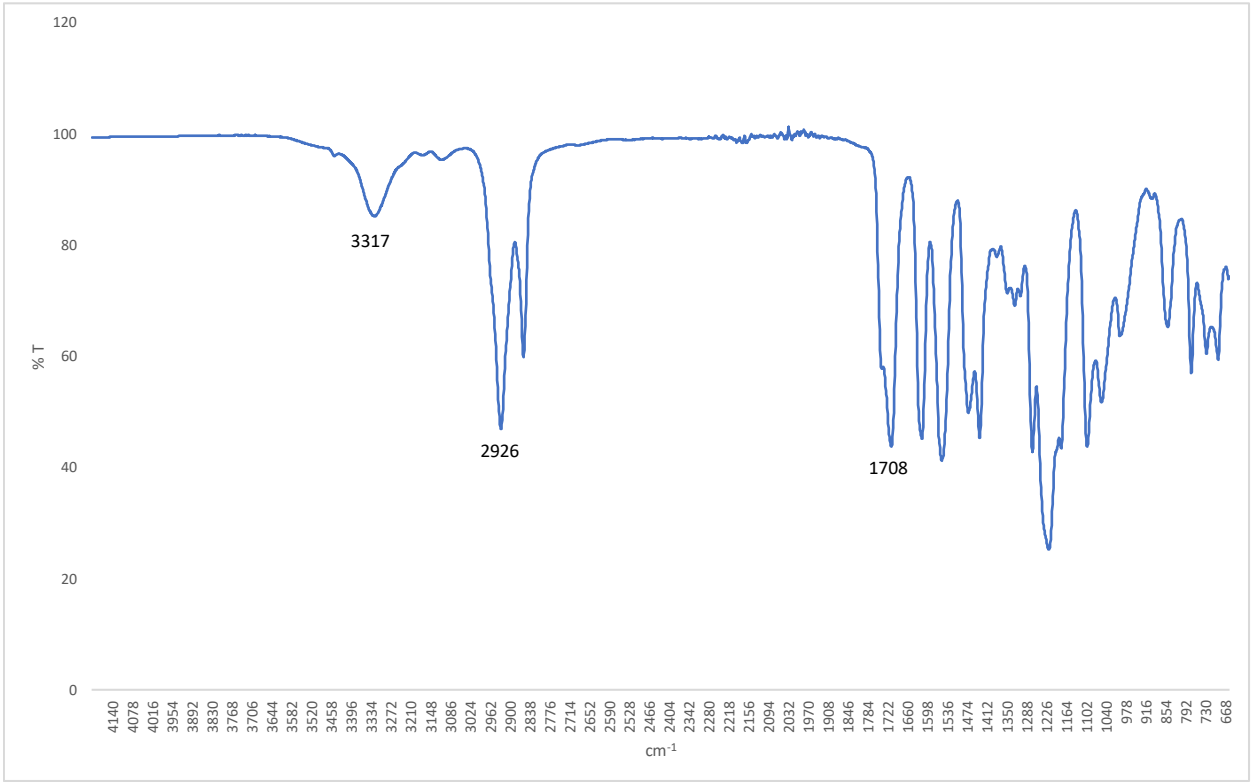

Figure S49. FT-IR spectrum of **G2W**.

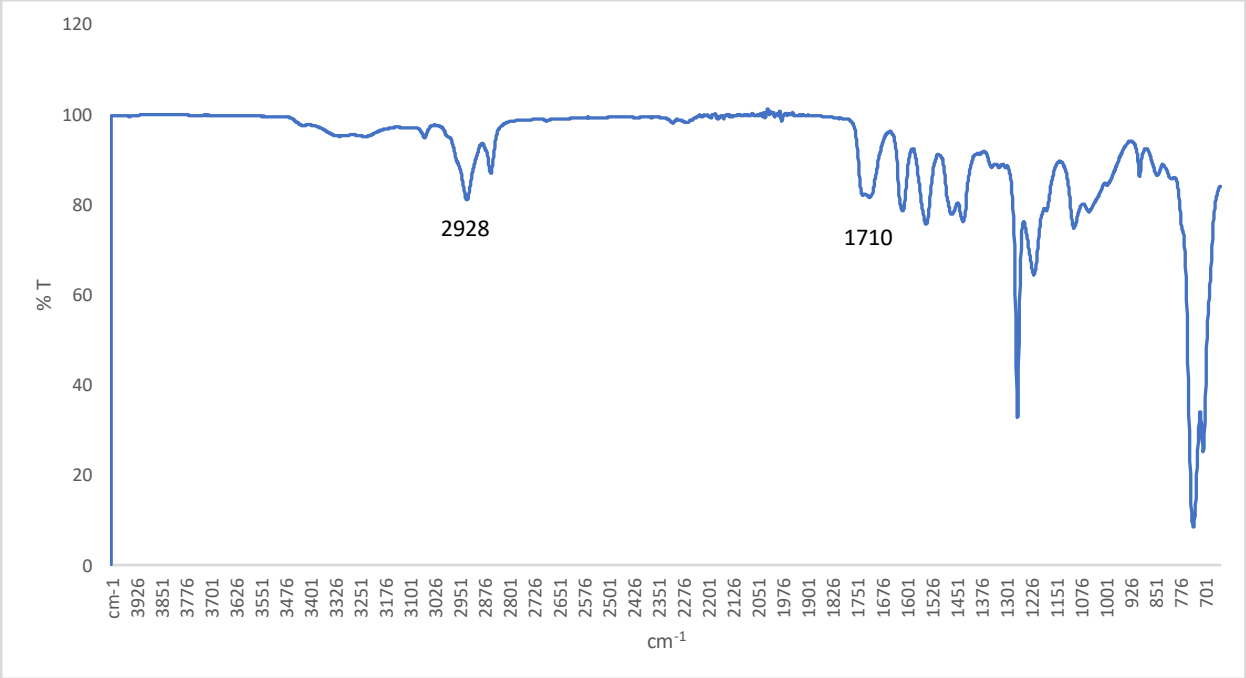

Figure S50. FT-IR spectrum of **G2D**.

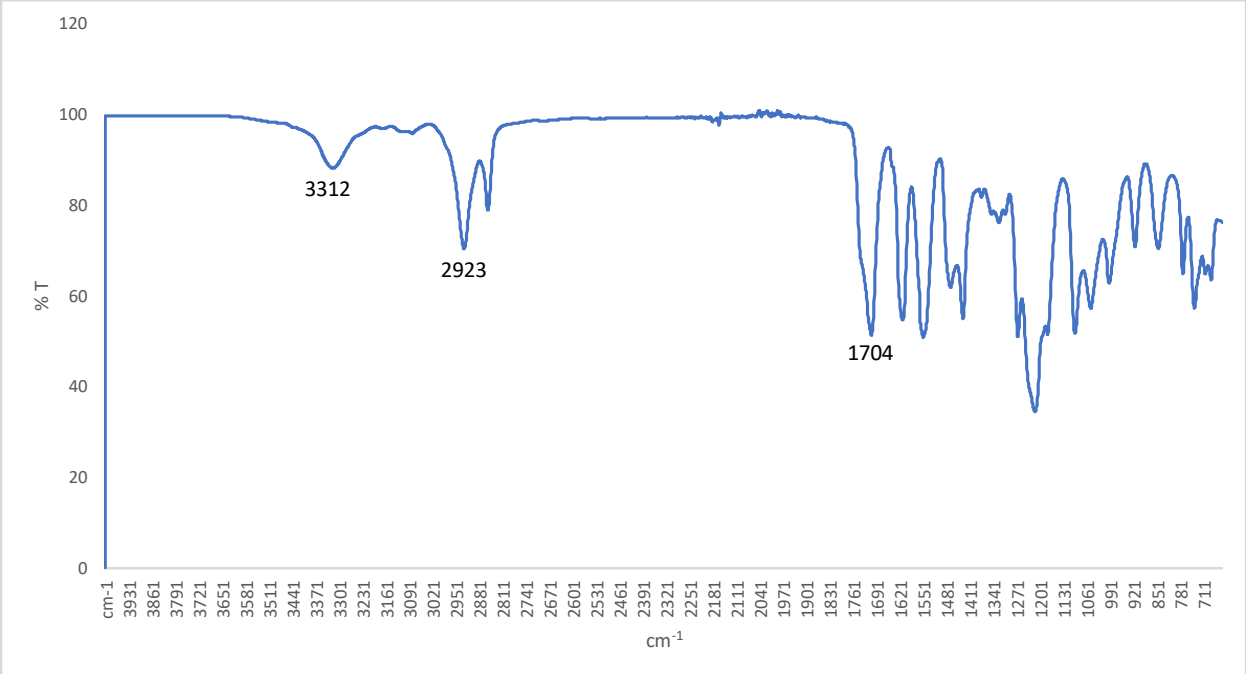

Figure S51. FT-IR spectrum of **$(G3W)_{ene}$**.

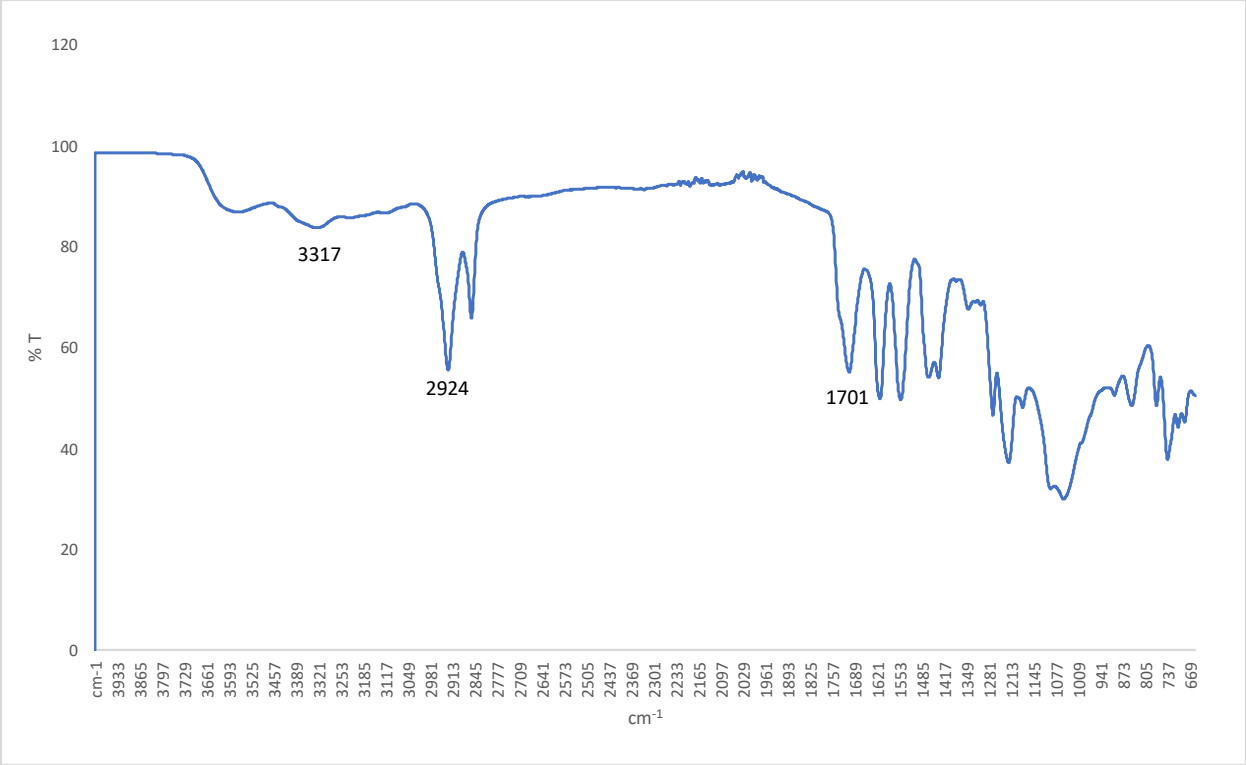

Figure S52. FT-IR spectrum of **G3W**.

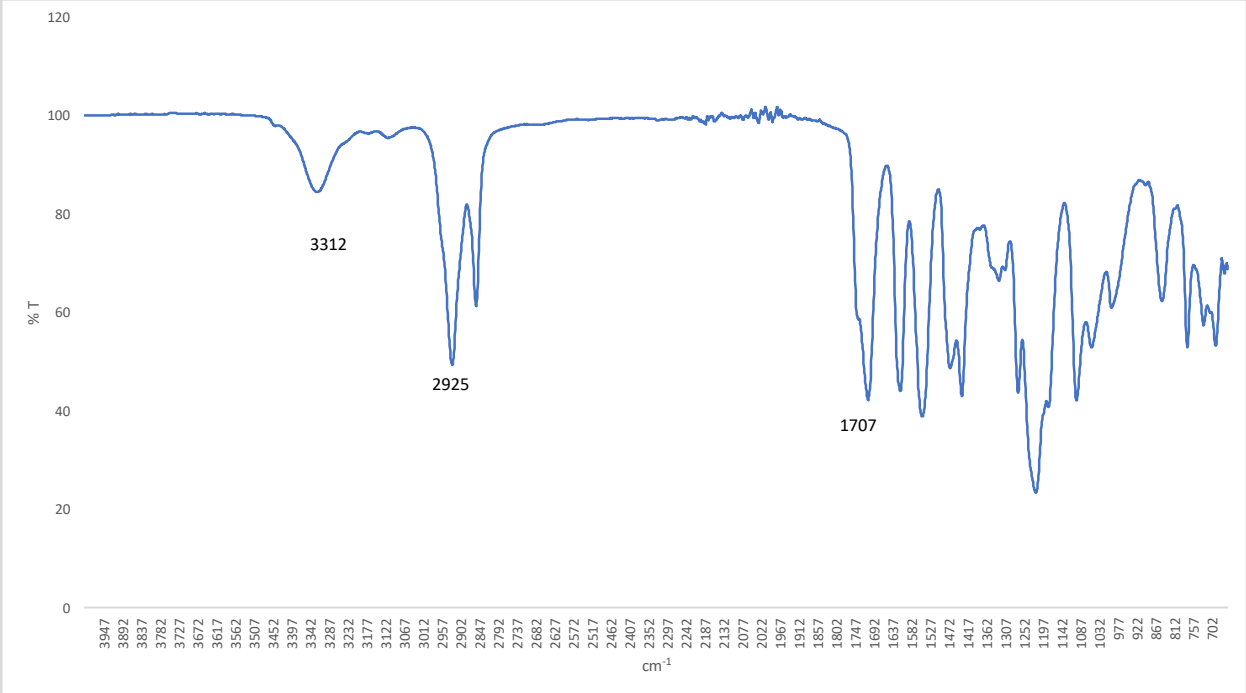

Figure S53. FT-IR spectrum of **G3D**.

6. UV-Vis and fluorescence study of G3 dendrimer (G3D).

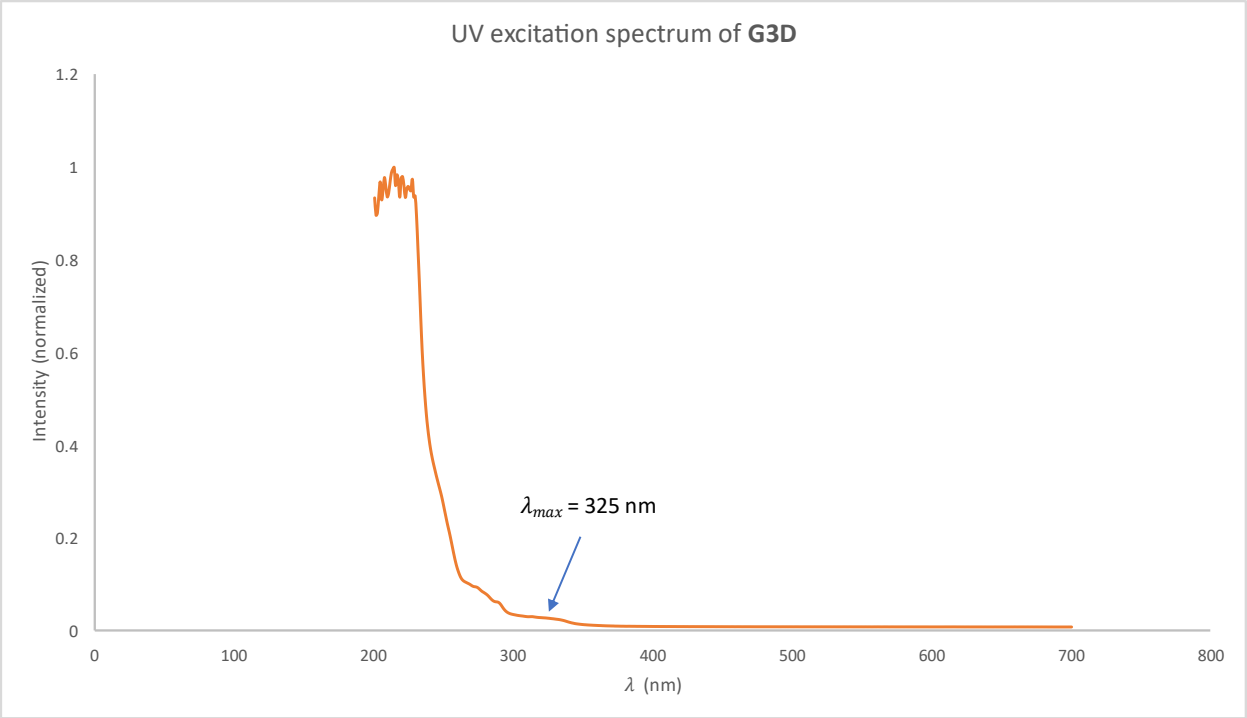

Figure S54. UV-Vis spectrum of **G3D** (measured at 1.3 mM concentration).

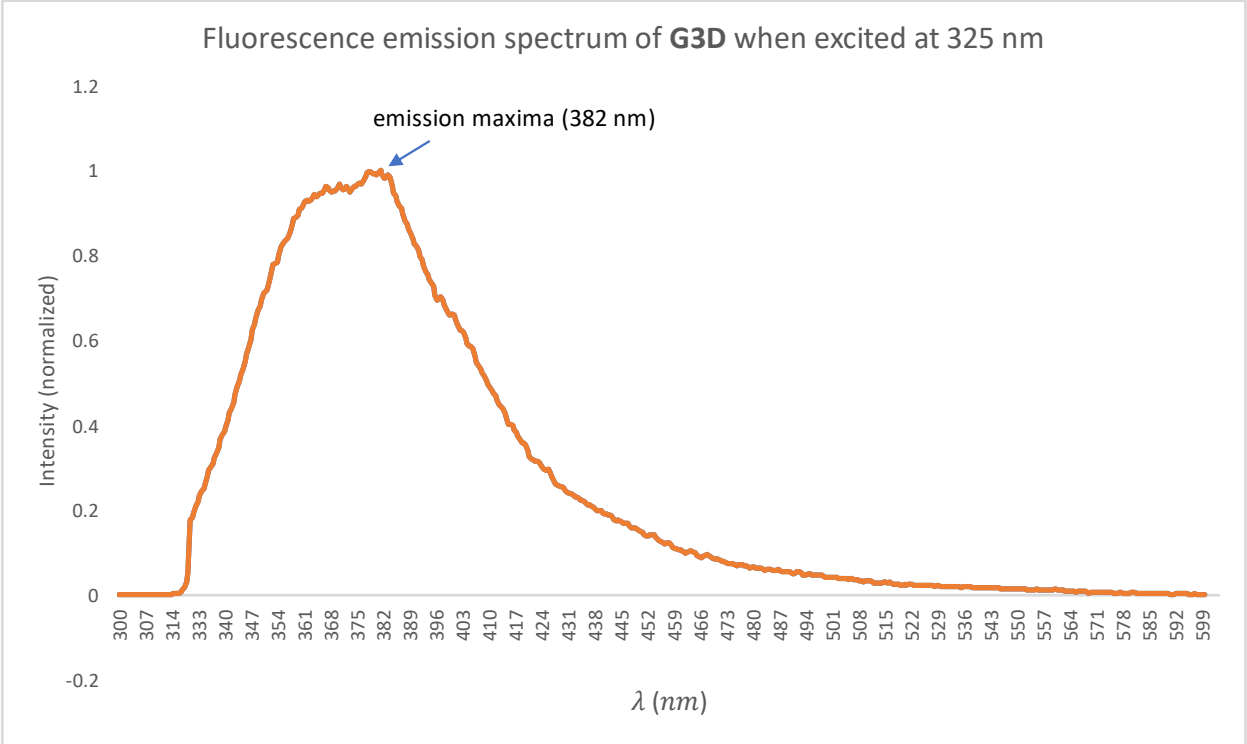

Figure S55. Emission spectrum of **G3D** (measured at 1.3 mM concentration). The data of the excitation portion (317 nm – 331 nm) are removed for clarity.